AFRL-SR-AR-TR-02-

REPORT DOCUMENTATION PAGE

0338

1. REPORT DATE (DD-MM-YYYY)	2. REPORT TYPE	3. DATES COVERED (From - To)
24-06-2002	Final Report	03-01-98 to 5-31-01

4. TITLE AND SUBTITLE
Compliant Substrate For Mid Infrared Wavelength Region

5a. CONTRACT NUMBER

5b. GRANT NUMBER
F49620-98-1-0328

5c. PROGRAM ELEMENT NUMBER

6. AUTHOR(S)
Dr. Shanthi Iyer

5d. PROJECT NUMBER

5e. TASK NUMBER

5f. WORK UNIT NUMBER

7. PERFORMING ORGANIZATION NAME(S) AND ADDRESS(ES)

Dr.Shanthi Iyer
Department of Electrical Engg
536 McNair
Hall,Greensboro,NC-27411

8. PERFORMING ORGANIZATION REPORT NUMBER

9. SPONSORING / MONITORING AGENCY NAME(S) AND ADDRESS(ES)
USAF/AFRL
AF Office Of Scientific
Research,801 N Randolph St,
Room-732, Arlington,
VA-22203-1977

10. SPONSOR/MONITOR'S ACRONYM(S)
DOD-Air Force/AFOSR/Bolling

11. SPONSOR/MONITOR'S REPORT NUMBER(S)

12. DISTRIBUTION / AVAILABILITY STATEMENT

Unlimited

20021031 027

13. SUPPLEMENTARY NOTES

14. ABSTRACT

The work in this project was focused on the growth of GaSb epilayer on a compliant layer by Molecular Beam Epitaxial (MBE) technique. A novel approach using the low temperature melting interlayer and a thin strained layer on top was investigated for compliancy. The structures examined consisted of GaAs host substrate, InSb as the low melting point interlayer, thin (Ga,Al) Sb layer, followed by thick GaSb overlayer. Growth results and characterization of these structures using various in-situ and ex-situ techniques are presented here.

Amongst the different interlayers examined, InSb/GaSb(grown at low temperature of 400°C) interlayer was found to be the most successful interlayer. The significant stress arising from the mismatch was accomodated by the interlayer, leading to reduced dislocation density ($<10^7$ cm^{-2}) in the GaSb overlayer.

Electronic properties of heteroepitaxial undoped and n-doping using SnTe source in InSb epilayers have been explained using the multichannel condcution process. High carrier (77K) mobility of 94,098 cm^2/V-sec on lightly doped samples has been achieved. Photoreflectance study of n-GaSb at $E_0+\Delta_0$ transition energy has also been the subject of detailed investigation. The dependence of $E_0+\Delta_0$ transition energy on the doping levels has been analyzed by including the effects of band filling, band gap renormalization, and tail states.

15. SUBJECT TERMS
Compliant layers, compliant substrate, Lattice engineered substrate,dislocation density, MBE, antimonide compounds,photoreflectance, mobility spectrum, interlayers, electrical transport properties.

16. SECURITY CLASSIFICATION OF:			17. LIMITATION OF ABSTRACT	18. NUMBER OF PAGES	19a. NAME OF RESPONSIBLE PERSON
a. REPORT	b. ABSTRACT	c. THIS PAGE			Dr.Shanthi Iyer
U			UU	53	19b. TELEPHONE NUMBER (include area code) (336)-334-7761 Ext:220

Table Of Contents

707°C] layer, followed by thick GaSb overlayer. Heteroepitaxial growth of InSb on GaAs was also a subject of detailed investigation. During the initial period the grant, MBE system developed some major problems associated with the transfer alignment and substrate manipulator system, hence, significant effort was also focused on low temperature photoreflectance study of GaSb during the period when the MBE system was not operational. These projects also formed the continuation of the previous project funded by AFOSR. This change was done in consent with the technical monitor Major Daniel Johnstone.

II. RESEARCH ACTIVITIES AND MAJOR ACCOMPLISHMENTS

The research activities during this period have been broadly classified into the following categories.

- Comprehensive study of GaSb epilayers grown on InSb compliant layer

  Systems consisting of different interlayers studied were:
  GaAs/InSb /GaSb (LT), GaAs/InSb/AlSb/GaSb (LT), GaAs/InSb/AlSb/ [GaSb (50° A) /AlSb (50° A)] [GaSb (LT) refers to the growth of GaSb at low temperature of 400° C]
  - In situ RHEED evaluation of the growth
  - Evaluation of surface morphology
    - High-resolution x-ray diffraction studies
    - Plan view and cross sectional transmission electron microscope studies

- MBE growth of undoped and n-InSb epilayers using SnTe source
  - Growth study
  - Electrical transport studies in both undoped and doped InSb
    - Temperature and magnetic field dependence of Hall and resistivity measurements
    - Various multicarrier conduction analysis

- Photoreflectance studies of Te-doped GaSb at the $E_0+\Delta_0$ transition
  - Temperature dependence of PR response on the bulk and homoepitaxially grown Te-doped GaSb
  - Line shape analysis of the PR spectra
  - Evaluation of the temperature dependence of $E_0+\Delta_0$ transition energy using band filling and band gap renormalization

Major accomplishments in each of above research activities are summarized below

- Comprehensive study of GaSb epilayers grown on InSb compliant layer
  - Significant reduction in the dislocation density ($<10^7/cm^2$) was obtained

on GaSb overlayer grown on InSb/GaSb (LT)
- Excellent structural quality as determined by transmission electron microscopy
- Difference in the growth mode of III-Sb on GaAs and AlSb on InSb

This work will be shortly communicated to J. Appl. Phys. and the details are described in sec. A.

- Heteroepitaxial growth of undoped and n-InSb epilayers

  - Heteroepitaxial growth of undoped InSb of good quality by MBE
    - X-ray FWHM 98 arc-sec on a 5 μm thick epilayer
    - Hall Mobility 65K (cm^2/V-s) @ $1.9x10^{16}/cm^3$
    - The undoped samples exhibited three electron channels attributed to the bulk (the high mobility channel), the surface accumulation layer and a defective and conductive layer at the InSb/GaAs interface, while the doped sample showed only two channels.

  - SnTe is a good candidate for n-type dopant in MBE grown InSb
    - Wide doping range $2x10^{16}/cm^3$ - 3.2×10^{18} cm^{-3}
    - Variation in x-ray FWHM 140-200 arcsec
    - High 77K-mobility 92,000 cm^2/V-sec for low doped InSb
    - Hall mobility (77K) - 20K cm^2/V-s at 1.3×10^{18} cm^{-3}

J. Appl. Phys. accepted for publication in June issue of 2002 and attached in sec. B.

- Photoreflectance Studies of Te-doped GaSb at the $E_0+\Delta_0$ Transition

  - First reports on the PR study on n-GaSb
  - Band to band transition at a 3-D critical point
  - Correlation of the shift in transition energy to the carrier concentration using many body effects
  - In undoped bulk GaSb, the high concentration of intrinsic defects prevent, via Fermi level pinning, the electromodulation mechanism

J.Appl. Phys. 87,2336 (2000) and attached in sec. C.

- Lateral oxidation of Ga(As,Sb)/Al(As,Sb)/InP.

  - This work has been carried out by University of California at Santa Barbara

A final report submitted by UCSB is attached in sec. D

Following is the detailed description of the above research work.

A. Comprehensive Study of GaSb Epilayers Grown on InSb Compliant Layer

(a) Introduction

The III-V semiconductor-based heterostructures have been of great importance due to their wide range of applications in both optoelectronic and electronic devices. In particular, thin layers of Sb-based compound and alloys have found considerable interest because of potential applications in III-V semiconductor-based infrared optoelectronic devices. GaSb is one of the substrates for these applications for it is not as rugged as the GaAs substrate. Therefore from a technology point of view, heteroepitaxy of GaSb on GaAs substrate is advantageous for monolithic integration of GaSb devices on GaAs substrates in microelectronics and infrared detector array fabrication. The lattice mismatch between GaSb and GaAs is 7.5%. Strain energy reduction in the lattice is accommodated by the production of an array of misfit dislocations at the GaAs/GaSb interface. This results in threading dislocations propagating through the epilayers with a concentration of about 10^8 cm^{-2}, for a 1μm thick layer [4], which impacts the performance of devices. Reduction of the threading dislocation density in the mismatched layer has been one of the areas that have been extensively studied.

One of the ways to control the strain in a lattice-mismatched overlayer is by accommodating part of the strain in a layer with weak interfaces, i.e. weakly bonded compliant layers. This concept was introduced by Chavarkar et al. [3] when they studied the InGaAs/AlAs/GaAs layers and the substrate is known as lattice engineered substrate. Recently, Romanov and Speck [5] have attempted to explain the reduction in the threading dislocation density by different techniques under a common framework using the model of relaxation enhancing interlayers.

In this work. we have investigated a novel approach based on the above concept, using an interlayer that has a low melting temperature relative to both the thin mismatched-strained layer (grown on the interlayer) and the underlying substrate. When the growth is carried out close to the melting point of the interlayer, the interlayer may become soft enough to accommodate misfit strain in the strained overlayer. As the bonding between the interlayer and the strained layer becomes weak, enhanced strain relaxation is likely to occur by easier misfit dislocation formation at interlayer/strained layer interface. Thus, strain relaxation in the thin strained layer without generation of

high density of threading dislocations can be achieved. The relaxed thin layer can then be used as a template for further epitaxial growth. In our work, InSb has been used as the low melting temperature interlayer to provide the necessary strain relaxation for the GaAs/ GaSb lattice mismatched system under study.

(b) Experimental Details

The GaSb samples described in this work were grown in an EPI 930 solid source MBE system. The sources used were elemental In (7N), Sb(6N5) ,Ga (8N) and As (7N). The cracking zone temperature of 900°C was used, for both As valved cracker cell and Sb cracker cell, to obtain the dimer species. Commercial, nominally flat, semi-insulating, undoped epi-ready GaAs (100) wafers were used for the substrate. Growth temperatures were monitored mainly by the pyrometer though the temperature indicated by the thermocouple (placed at the rear of the substrate manipulator) was used as a guideline to set the temperature of the molyblock. An ionization gauge positioned at the substrate was used to measure the beam equivalent pressure of aluminum, arsenic, gallium, indium, and antimony fluxes. The fluxes of the group III elements were calibrated using the RHEED oscillations and were set for a growth rate of 0.7 μm /hr for all the binary growths and these were confirmed on some of the samples using the cross -sectional SEM photographs.

The in-situ oxide removal from the surface consisted of outgassing at 200^0C in the load lock chamber followed by outgassing in the growth chamber under As overpressure for 20 min at 620^0C, until a bright diffraction pattern is seen on the RHEED screen, indicative of the completion of the desorption process. An initial 0.2–0.3 μm of buffer GaAs layer was grown on the substrate at 580°C with a (2x4) reconstruction observed by reflection high energy electron diffraction (RHEED). Then the substrate temperature was lowered to less than 400°C with the As shutter closed, in order to reduce the background intensity of As in the growth chamber and then bringing the substrate temperature to the desired growth temperature. The shutters of In and Sb cells were opened for InSb growth, while the surface was monitored continuously by RHEED followed by other interlayers.

We grew a series of samples on GaAs substrate with different interlayers with the first interlayer in all the cases being InSb and final terminating with thick GaSb layer. The thin interlayer grown on top of InSb examined were GaSb (grown at 400^0C referred to as GaSb (LT), the samples 1xxxxx, 2xxxxx, 3xxxxx), GaSb/AlSb (samples 4xxxxx), AlSb/$[AlSb/GaSb]_{10}$/(samples 4xxxx). We also grew a few samples (5xxxxx) where GaSb was grown directly on to the GaAs substrate and on AlSb buffer layer as the reference materials for comparison. The schematic of the layer structure is shown in Fig.1 and the details of the MBE growth are listed in Table 1.

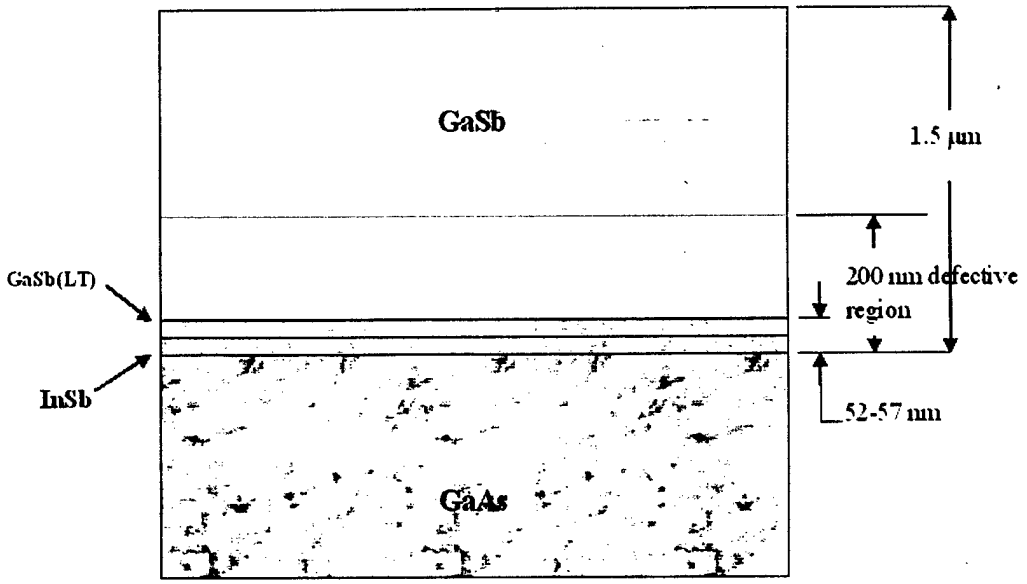

FIG.1. Schematic of GaAs substrate-interlayers-GaSb overlayer structure.

TABLE 1. The samples grown under various conditions and their x-ray characterization

Sample	InSb/ GaSb (LT)			GaSb Overlayer			X-Ray	
	Growth Temp (C)	*Growth Time (sec)*	*Est. Thickness (Å)*	*Growth Temp (C)*	*Growth Time (min)*	*Thickness (nm)*	*FWHM arc-sec*	*Peak Count (cps)*
1071700	350	36/18	70/35	470	68	793	577	1146
1041900	403	36/18	70/35	488	20	233	No signal	26
1072400a	405	60/120	120/230	487	20	233	1140-1440	190
1072400b	416	60/120	120/230	487	20	233	1640-1919	76
2080300	413	60/120	120/230	470	60	700	1500-1600	161-567
2111400	414	60/120	120/230	471-478	65	758	865	1378
2112800	413	60/120	120/230	480-482	69	805	1854	911
2081000	412	60/120	120/230	482	65	651	935-960	1155
2080800	413	120/60	230/120	481-491	40	467	1111	1036
2081100	413	60/120	120/230	475-501	45	524	2000-2300	340
3091400	411	120/120	230/230	483	120	**1229;1489**	519	5942
3101200	413	60/120	120/230	482	150	**1327;1391**	543	5517
3101700	413	60/120	120/230	500	150	**1448;1690**	700	4000
3110200	413	60/120	120/230	501-504	161	1878	1174	2074
	InSb/AlSb/GaSb (LT)							
4020701	425/475/475	240/120/120	460/120/120	510	150	**1827;1845**	570	5395
4022601	410/450	240/60/120	460/120/120	520-500	150	1750	2077	850
	InSb							
4020501	424	240	460	510	2/90	**893**	809	2503
	InSb/AlSb			**$(SL)_{10}$ – GaSb Overlayer**				
4022301	411/449	240/60	460/120	516-500	150	1750	915-978	3036
4030701	412/451	240/60	460/120	510/520-500	150	**1330; 1334**	514	6604
	AlSb		**Reference Samples**					
5020900	530		233	506		1690	202	2197
5030201	530	120	233	500	127	2117	212	10808
5021500				519		977	126-445	733
5021901				504	150	1750	233	10397
	InSb							
616	370		4.0μm				236	

In-situ characterization was carried out utilizing 15KeV RHEED gun with image, acquisition and analysis system (RHEED). Ex-situ examination of the surface morphology was carried out using Nomarski phase contrast microscopy, scanning electron microscopy and atomic force microscopy (AFM). High resolution x-ray diffraction (HXRD) was used to determine the lattice mismatch and reciprocal lattice mapping. Double axis and triple axis $\omega/2\phi$ on (004) and (224) orientation scans on couple of samples were carried out by Bede Scientific personnel. Transmission electron microscopy was carried out to determine the nature of dislocations at the interface.

(c) Results

Considering the wide range of growth parameters such as the growth temperature, the thickness of the epilayer and the constitution of the interlayer that can influence the ultimate dislocation density the results are first presented for optimizing the growth temperature and thickness followed by the dependence on the type of the interlayer for each characterization measurement.

i. RHEED Measurements

Figure 1 shows the sequence of RHEED patterns observed on the <010> azimuth during the growth. On initiation of the InSb growth the RHEED pattern remains unchanged, i.e. (2x4) as that of GaAs for about 3-4 seconds. Thereafter a bright diamond transmission pattern appears indicative of 3D-island growth. It is also consistent with the intensity oscillations observed (see Figures 2a-2d) and the invariant d-spacing during this period (as indicated later in Figure 4). Similar intensity oscillations are observed for the GaSb and AlSb growth on GaAs as well, though the transient durations are somewhat longer and variation in amplitudes are different from those observed on InSb layers. Thereafter the intensity of the specular spot decreases with time. However, for AlSb growth reconstruction does not change, but the growth results in an initial marginal decrease in intensity within 3-5 seconds followed by rapid increase of the intensity of the specular and 1/3 integral orders.

Figures 4a-4d exhibit the variations in FWHM of the Bragg spots/streaks at the beginning of each layer growth, which is indicative of the surface roughness of the growth. III-Sb growth on GaAs exhibits a transient for first few seconds and comes back quickly to the value before the onset of the epilayer growth, while in the case of AlSb growth on InSb the recovery period is much larger, in tens of seconds.

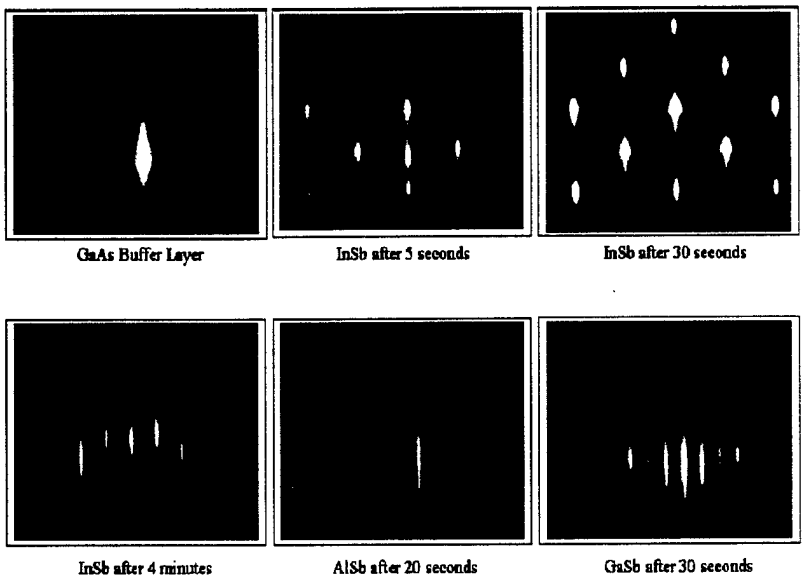

Fig. 2. Evolution of RHEED reconstruction with time, during different layer growths.

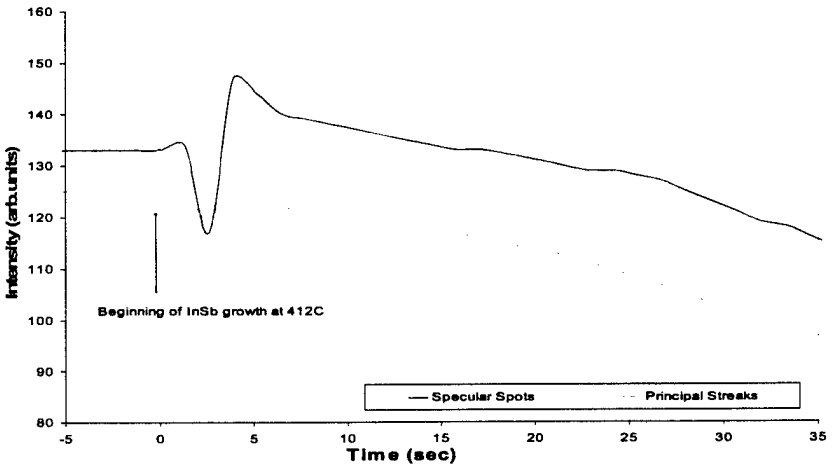

Fig.3a. Variation in intensity at the beginning of InSb growth on GaAs for sample #4022801.

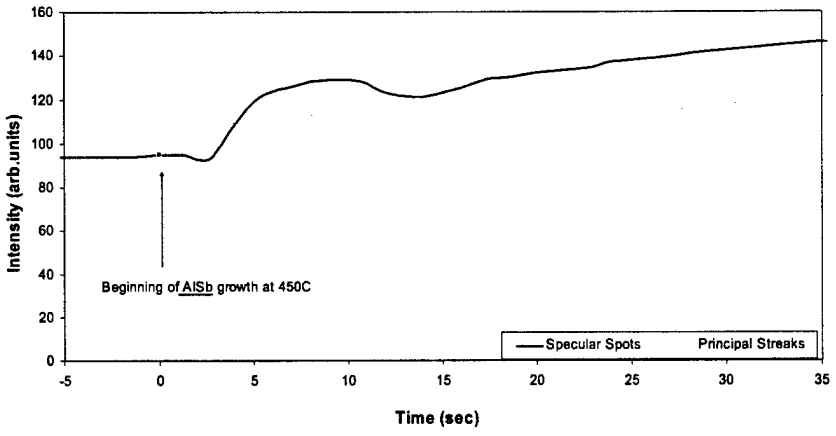

Fig.3b. Variation in intensity at the beginning of AlSb growth on InSb sample (#4022801)

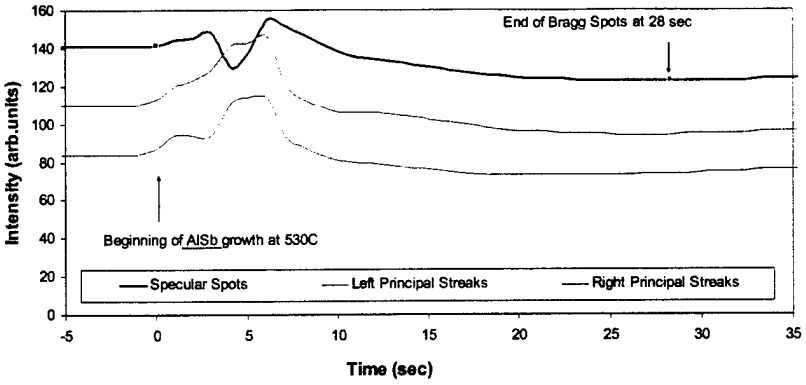

Fig.3c. Variation in intensity at the beginning of AlSb growth on GaAs (reference material;sample#5030201)

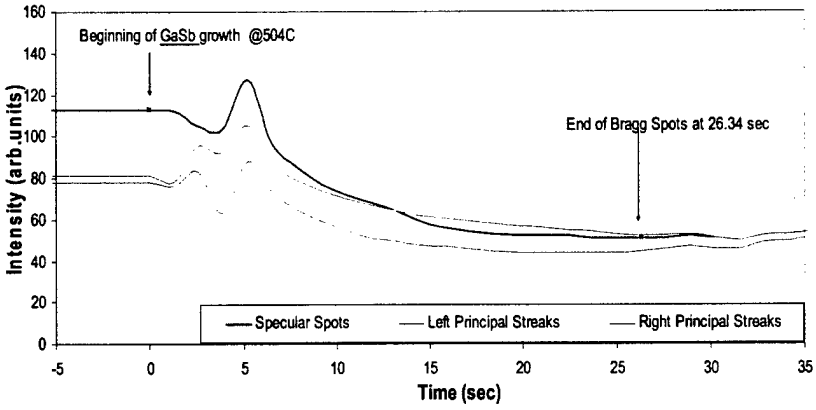

Fig.3d. Variation in intensity of GaSb grown on GaAs (reference material;sample #5021901)

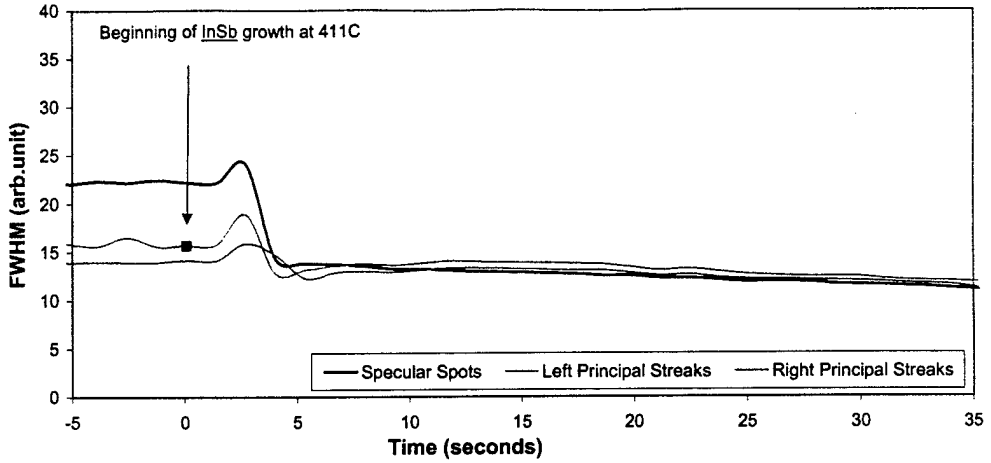

Fig.4a. Variation in FWHM at the beginning of InSb growth on GaAs (sample #4022301)

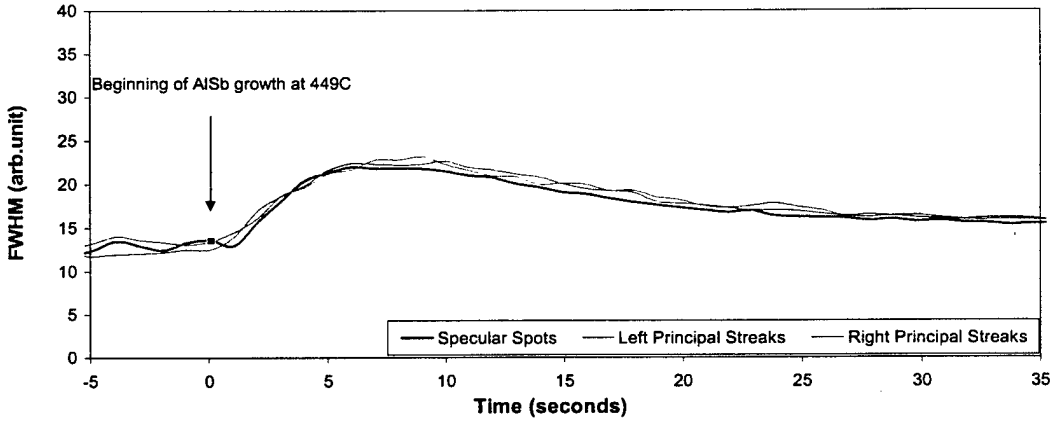

Fig.4b. Variation in FWHM at the beginning of AlSb growth on InSb (sample #4022301)

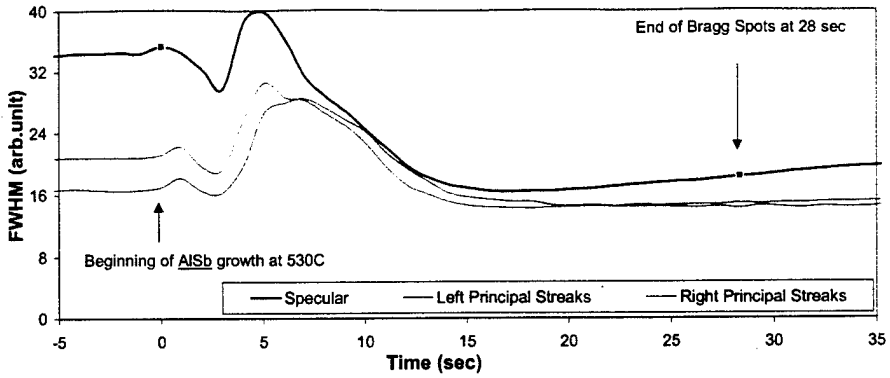

Fig.4c. Variation in FWHM at the beginning of AlSb growth for reference material GaAs/AlSb/GaSb (#5030201).

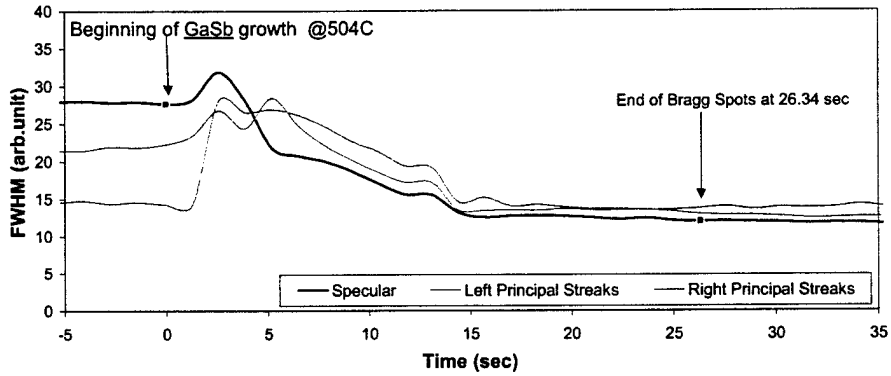

Fig. 4d. Variation in FWHM at the beginning of GaSb growth for reference material GaAs/GaSb (#5021901)

Figure 5 shows the changes in the lattice parameter with the initiation of the growth. Lattice parameter change is almost immediate for InSb growth on GaAs, within 3 seconds. However, the change in the lattice parameter of AlSb on InSb is somewhat more gradual over a period of 20-30 seconds. Often a strong half integer streak is observed when observed along <001> azimuth, which vanishes on increasing the Sb overpressure. Very little intensity modulation occurs as the growth proceeds, typical of strain relaxed surface, GaSb overlayer growth on all these layers exhibits extremely bright RHEED

pattern with even one third integer orders equally bright (see Fig.2). This is in contrast to GaSb either grown directly on GaAs or on AlSb buffer layer, where only the principal streaks are bright.

On increasing the growth temperature to 516°C -518°C, the intensity of the streaks decreases and appears to set the upper limit for the growth temperature of the GaSb overlayer, as beyond which the RHEED reconstruction almost disappeared. However, after few minutes of GaSb overlayer growth, the reconstruction reappears though somewhat broad and gradually becoming bright.

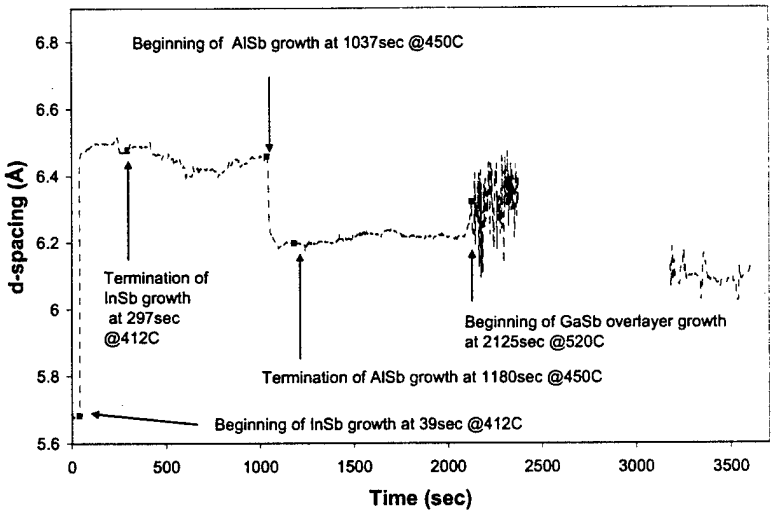

Fig.5. Variation of d-spacing with growth time for GaAs/InSb/AlSb/GaSb system

ii. Surface Morphology

Growth temperatures in the range of 350°C to 416°C (see Table 1) were investigated for the growth of InSb/GaSb interlayers. For temperatures below 400°C the GaSb overlayer grown exhibits square pits (see Fig.6a), which is significantly reduced when grown at temperatures around 413°C and the epilayer appeared to be atomically smooth as shown in AFM micrograph (see Fig.6b). The presence of square pits on (100) surface is indicative of high-density of threading dislocations. The local surface rms roughness of the sample grown at 413°C is about 1.7 nm, with mean roughness of 1.17 nm over a scanned area of 20x20 μm^2 which suggests atomically smooth surface. Hence, the growth temperature of InSb in most of the runs was kept above 410°C.We also found an upper limit to the overlayer growth temperature. For growth temperatures exceeding 500°C resulted in considerable degradation of the surface morphology as observed by Nomarski phase contrast microscope (see Fig.7).

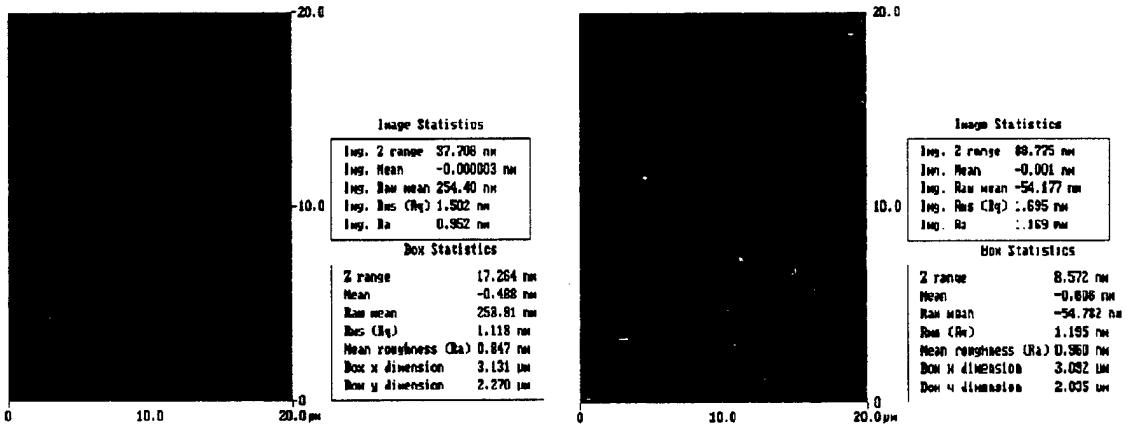

(a) (b)

Fig.6. AFM images of 0.2 µm thick GaSb layer grown on InSb/GaSb interlayer grown at (a) 400°C and (b) 413°C, respectively.

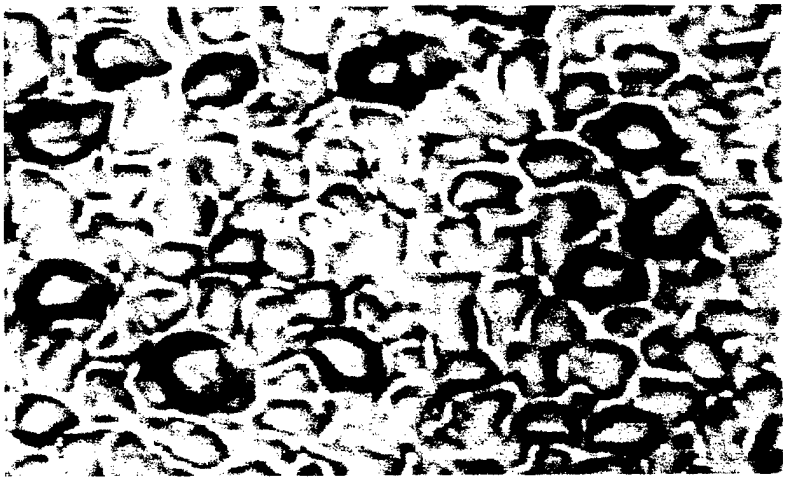

Fig.7. Nomarski phase contrast microscopy of GaSb overlayer grown on InSb/GaSb interlayer @ 504° C.

Both the reference samples GaSb grown directly on GaAs and the one grown on AlSb buffer layer exhibited faceted hillocks and the screw dislocation mediated growth as illustrated in Figs. 8a & 8b, respectively. These spiral mounds had screw orientation elongated in the [011] directions. The terraces were 45 nm wide in the [011] direction and 62 nm wide in the [011] direction. The step height was around 0.5 nm. This difference in terrace widths has been attributed[6] to the difference in anisotropy diffusion lengths of Ga adatom. With AlSb buffered layer the distance between the spiral mounds decreases and the neighboring spiral growth are in opposite sense. The width of the terracing decreased on both the directions to 3/4 th of its value to those grown directly on GaAs, namely 30 nm and 47 nm in two directions with a step height of 0.27 nm. This reduction in terrace width has generally been attributed[7] to the short diffusion length of the Al adatoms.

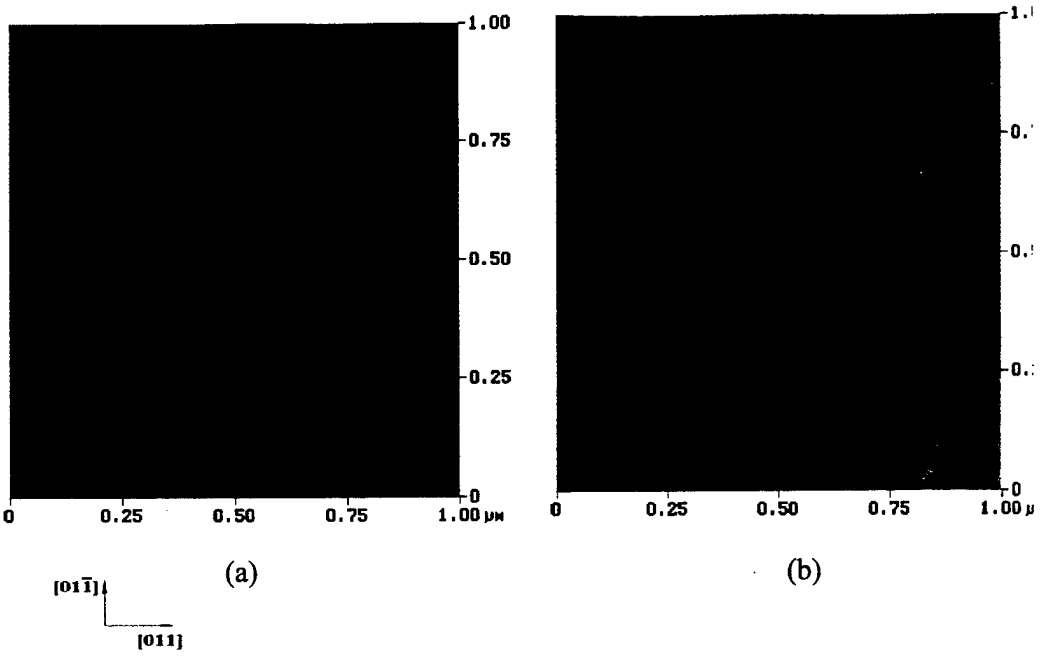

Fig. 8. AFM images of GaSb grown (a) directly on GaAs substrate and (b) on AlSb buffer layer

Growth of GaSb on GaAs/InSb/AlSb/$[(GaSb)/(AlSb)]_{10}$ interlayer exhibits crystallites of 2.6x2.6μm. All the crystallites have the same orientations and consist of similar mounds though the shapes are different. On the layers grown on InSb/GaSb (LT) we see similar observations except the features of the steps and terraces are not well defined. The step sizes were determined to be 0.4-0.5 nm, close to those observed on GaSb epilayers directly grown on GaAs. The rms surface roughness of both these layers is around 3-4 nm much larger than the 0.7-0.8 nm on layers grown directly on GaAs substrate.

The GaSb layers grown on InSb/GaSb(LT) interlayer exhibited mainly hillocks and stacking faults at only certain locations (Fig. 9a, 9b), and growth steps for thicker InSb interlayer (Fig. 9c,9d). However, when GaSb was grown on InSb/AlSb interlayer pronounced stacking faults with superimposition of spiral growth was observed (Figs. 10a &10b). The same sample was also examined using SEM to confirm that the lines were due to the stacking faults and not due to the cracks. The rms surface roughness of both these layers is around 3-4 nm much larger than the 0.7-0.8 nm on layers grown

directly on GaAs substrate. To determine the origin of stacking faults InSb directly grown on GaSb was also examined see Fig. 11. It exhibited stacking faults which has been generally attributed[8] to Sb segregation.

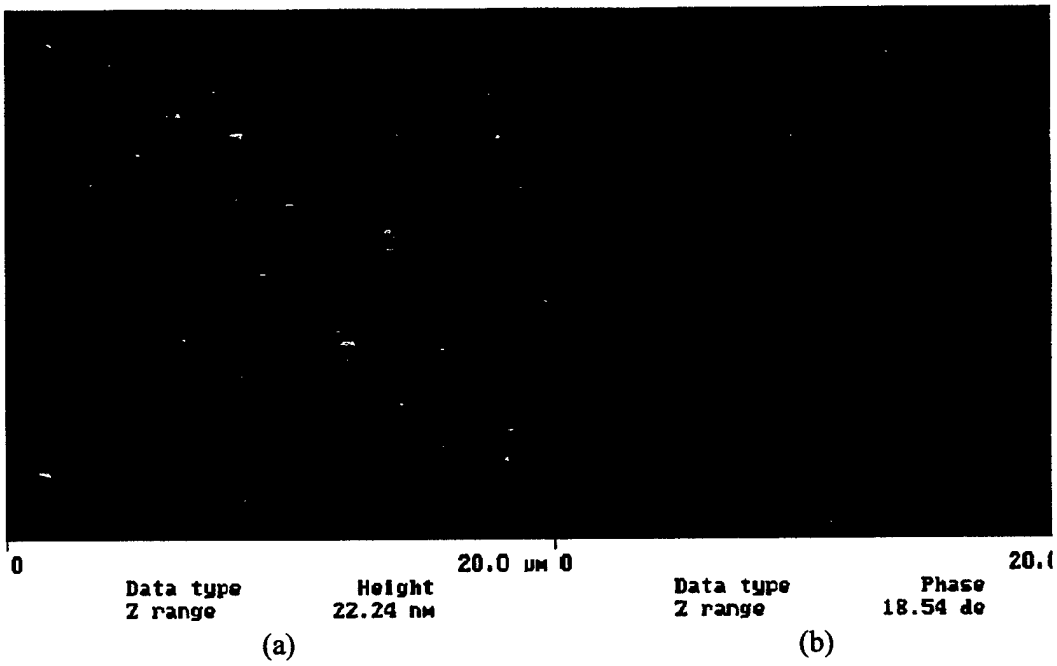

Fig. 9. AFM images of GaAs grown on InSb/GaAs(LT) interlayers for samples (b) #3101700 & (d) # 3091400. (a) & (c) are the corresponding phase contrast images,

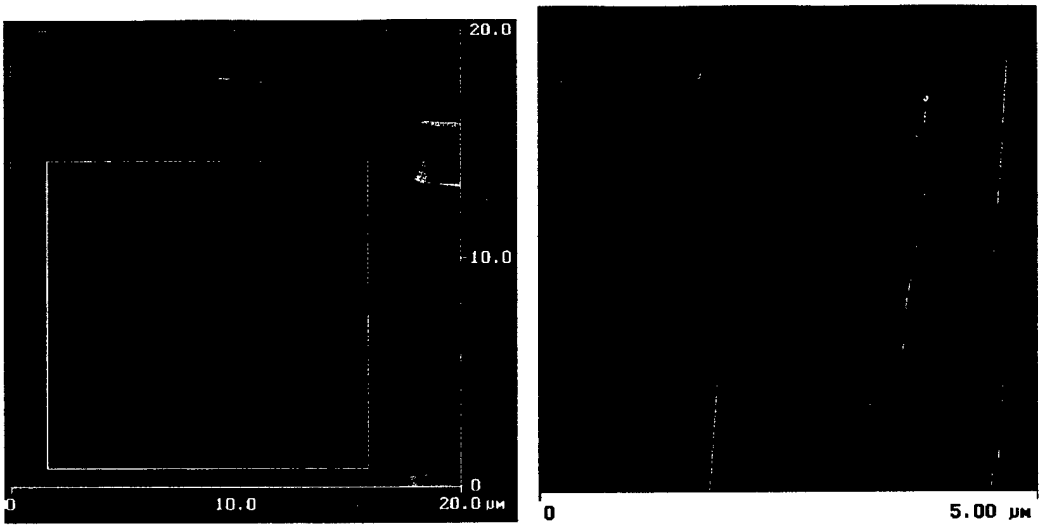

(a) (b)

Fig.10. AFM image of GaSb layer grown on InSb/AlSb interlayer (Sample #4030701), (a) is the phase contrast image of (b).

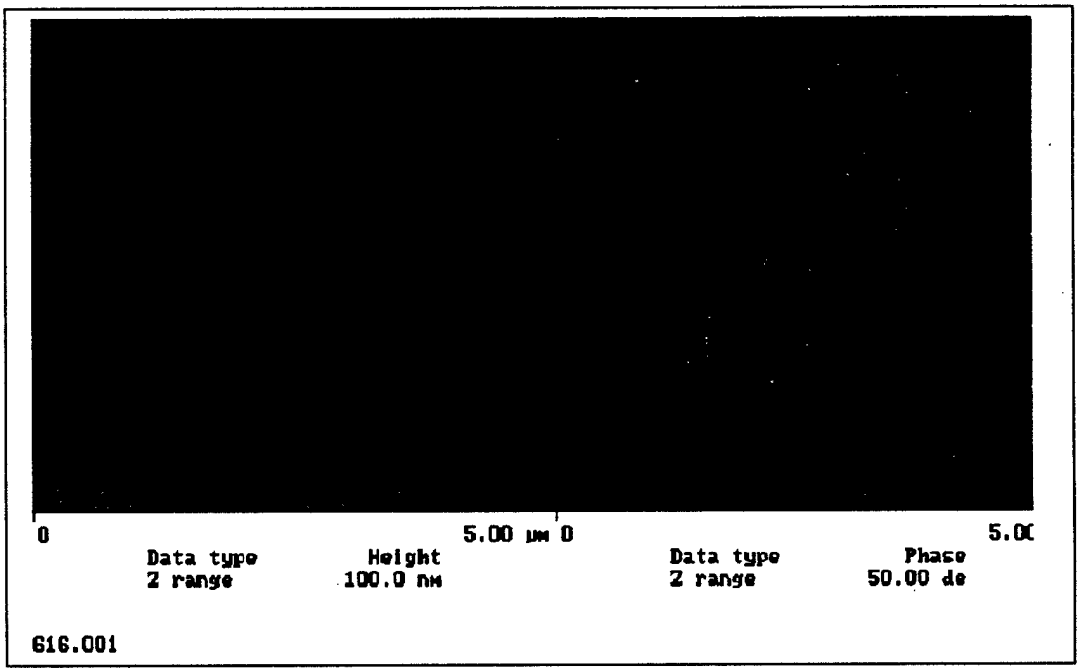

Fig. 11. AFM image of InSb grown on GaAs (sample # 616)

c. High Resolution X- Ray Diffraction Measurements

No strong dependence of the x-ray full width half-maxima (FWHM) on the type of the interlayer was observed. However, it was found to show a weak dependence on the substrate temperature of the GaSb overlayer (Fig.12), broader at higher growth temperatures. When the GaSb growth is carried out on InSb/AlSb interlayer, comparable x-ray FWHM is obtained at a slightly higher growth temperature of 510°C, however the lowest x-ray FWHM that could be achieved was still close to 600 arc-sec. Figure 13 exhibits the variation of FWHM of the x –ray-rocking curve with the thickness of the epilayer. The FWHM shows a decrease with increasing thickness of the epilayer as expected.

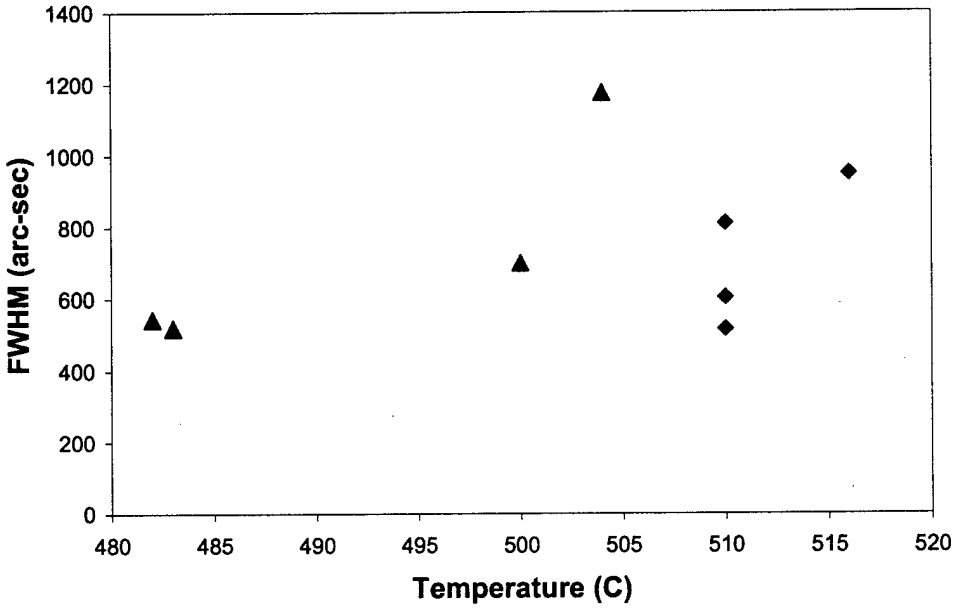

Fig. 12. Dependence of FWHM of the x-ray rocking curve on the GaSb growth temperature. The ▲ represents layers grown on InSb/GaSb. The ♦ represents layers grown on InSb/AlSb and SL. Layer thickness were in the range of 1750-2000nm.

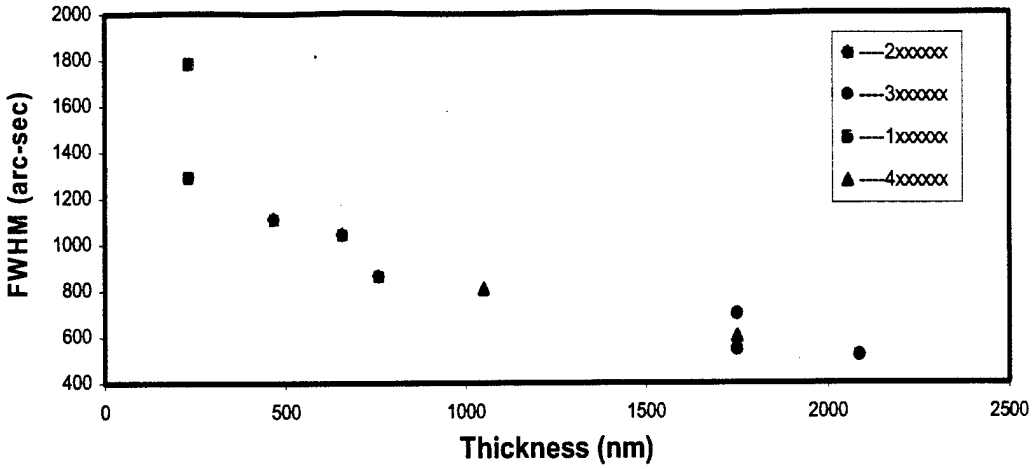

Fig. 13. Variation of FWHM of x-ray rocking curve with thickness of the GaSb overlayer.

A reciprocal lattice mapping of (004) and (224) orientations of GaSb epilayers (samples 309140 & 3101200) grown at 482°C on InSb/GaSb interlayers confirmed that the layers are fully relaxed as shown in Figure 14a. The FWHM of the layer peak along ω ($\approx q_{110}$ over this range) is approximately 500-520 arc sec and along $\omega/2\Theta$ ($\approx q_{001}$) is approximately 60 arc sec for both the samples. The large FHWM along ω suggests the presence of mosaic tilts in the samples. The (004) and double axis scans (at 0° and 180°) indicated no tilt for 3091400 and a 0.25° tilt between the layer and substrate for sample #3101200 (see Fig.14b). Finally, these layers were compared to the GaSb layers that were grown directly on a GaAs substrate and also to those grown on AlSb buffer layers. The FWHM of the layers on both of these samples were 250 arc-sec for a layer thickness of 1.7 μm, much lower than those grown on any of the interlayers.

On annealing the samples later in hydrogen ambient up to the growth temperature did not result in any change in the x-ray FWHM of the epilayer.

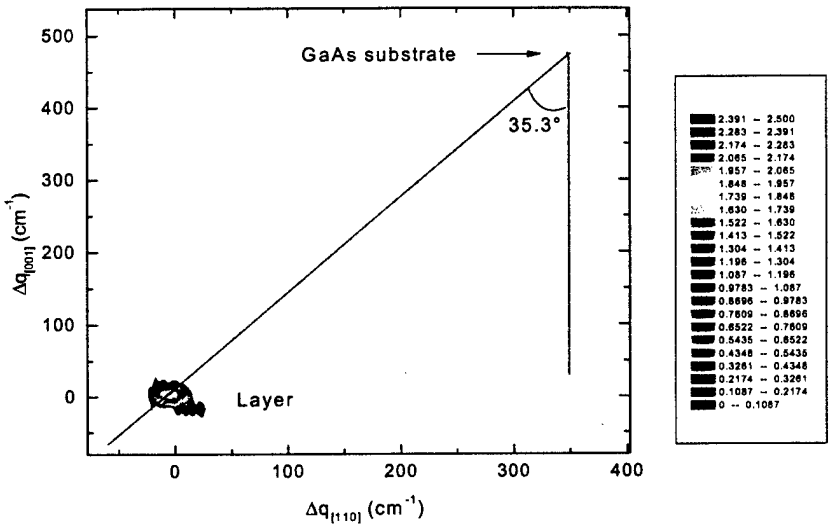

Fig.14a. (224) reciprocal space mapping for GaSb overlayer grown at 482 ^{0}C (sample #3091400).

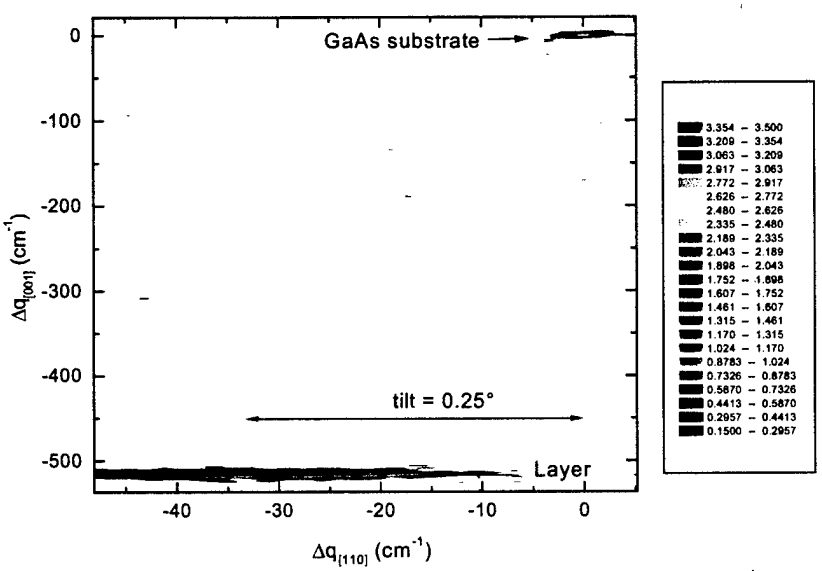

Fig.14b. (004) reciprocal space mapping for GaSb overlayer grown at 482°C with InSb (120Å) / GaSb (230Å) grown at 413°C (sample #3101200).

iv. TEM Measurements

Figures 15a & 15b show the plan view TEM images (bright field, dark field) of one of the samples (#1041900) that was grown when we started this project. The specimen was loaded bottom-side up with the growth surface pointing down. The interlayers used in this sample were InSb and GaSb of very small thickness (36 Å) and (18 Å), respectively. It is clearly evident from the plan view that the sample is a very defective material and nature of the individual defects could not be resolved due to the GaSb layer being very thin. The corresponding selected area diffraction pattern, as shown in Fig.15c, exhibited satellite spots around the dominant bulk GaAs spot. These satellite spots can be attributed to the double diffraction spots, where the first beam diffracted in a crystalline layer acts as a secondary source, causing additional diffraction from the layer underneath, which in this case will be the interlayers. The presence of satellite spots in specified directions is indicative of the fact that the layer underneath is crystalline, with different specified orientations and lattice parameter different from that of the GaAs substrate. Thus both the images and the diffraction pattern suggest the island growth mode of specified orientations for the interlayers with the island size estimated to be of the order of 50 - 100 nm.

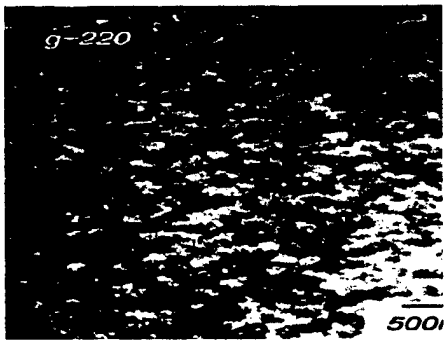

(a)

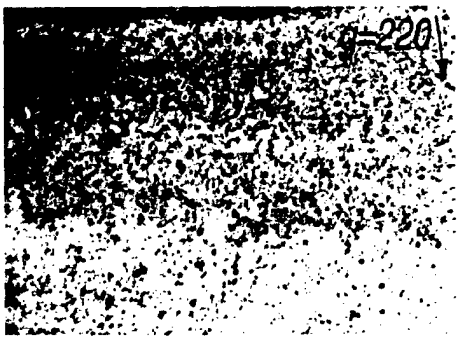

(b)

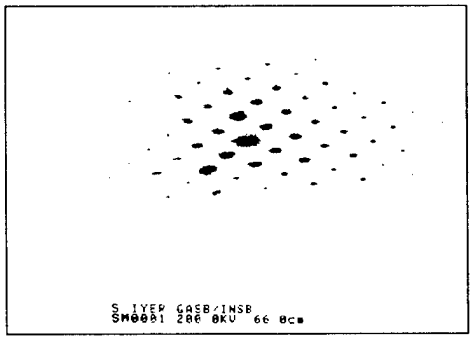

(c)

Fig. 15. Plan view TEM image of GaSb overlayer grown on InSb/GaSb interlayer (sample # 10419001)
(a) bright field, (b) dark field and (c) selected area diffraction pattern.

Figures 16 & 17 exhibit cross sectional TEM micrographs (taken at different locations) for the sample #3091400 (GaAs/InSb/GaSb(LT)/GaSb). This sample was chosen as its surface morphology did not exhibit any stacking faults and also had the lowest x-ray FWHM. Significant stress with extremely high dislocation density is observed near GaAs/InSb interface in the region of 52-57 nm which closely corresponds to the combined interlayer (InSb and GaSb (LT)) thickness (46nm based on the growth rate). The clear thin white lines can be seen in the weak beam dark field image Fig.17c, indicating the dislocation defects. The defect density remains high up to a thickness of 200 nm from the interface beyond which there is a significant reduction in the dislocation density (much less than 10^7 cm^{-2}). Figure 18 is the enlarged view of the interface exhibiting the Moiré fringes at the interface arising due to the large mismatch between the InSb and GaAs. The diffraction pattern at the interface (Figs. 19a &19b) shows the clear and bright satellite spots indicative of distinct two epilayers InSb and GaSb of different lattice constants. The cross fringes observed in high resolution TEM (Figure 20) is indicative of excellent structural quality of the GaSb overlayer. This was observed at different parts of the specimen.

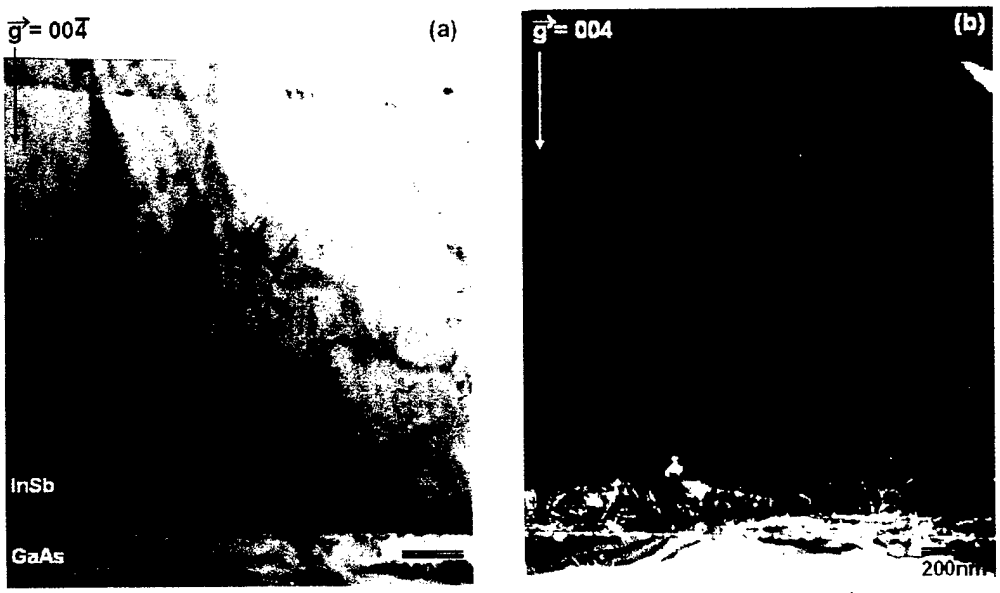

Fig. 16. TEM images of GaSb overlayer grown on InSb/GaSb(LT) interlayer
(a) bright field image and (b) weak beam dark field image for sample #3091400.

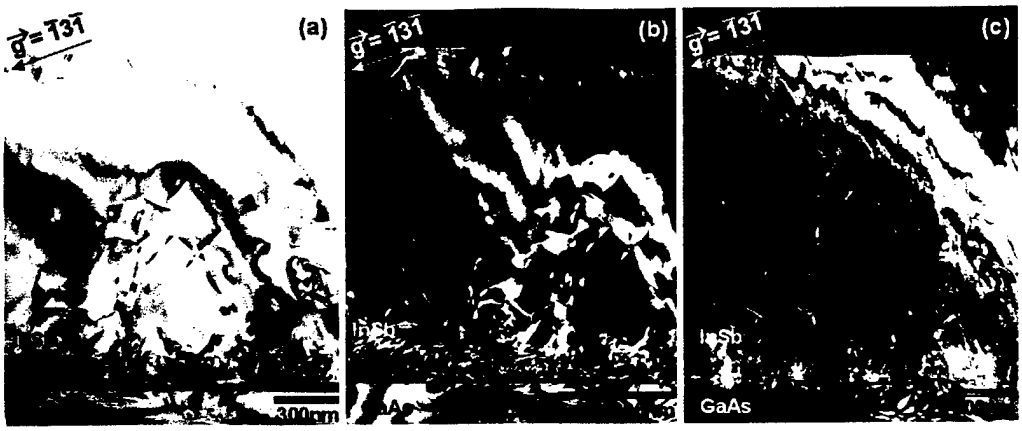

Fig 17. TEM images of GaSb overlayer grown on InSb/GaSb(LT) interlayer (a) bright field image, (b) dark field image and (c) weak beam dark field image for sample #3091400.

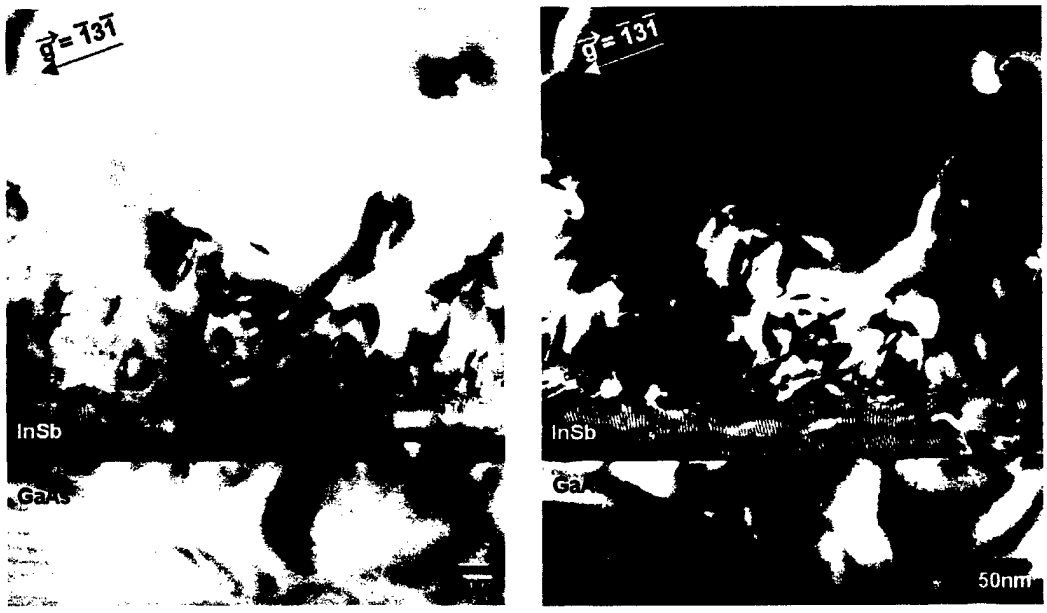

Fig. 18. TEM cross sectional images of GaSb overlayer grown on InSb/GaSb(LT) interlayer (a) bright field image and (b) dark field image (sample#3091400) exhibiting Moire fringes at the GaAs/ InSb interface..

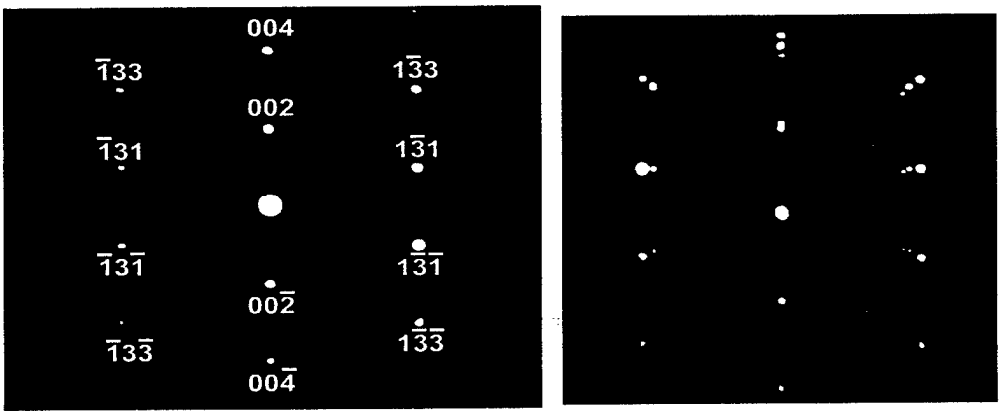

Fig. 19. Micro diffraction pattern of (a) substrate indicates the standard 13 spots indexed and (b) InSb/GaAs interface.

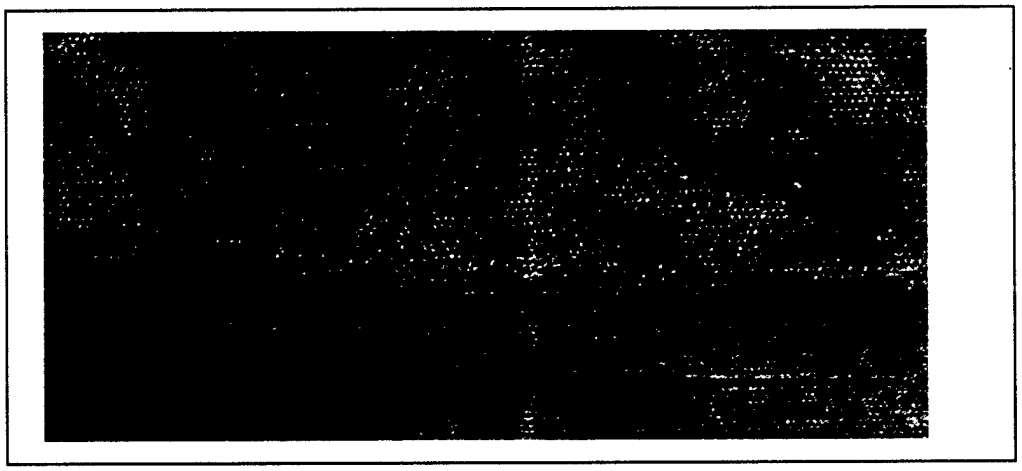

Fig. 20. High resolution TEM image of GaSb grown on InSb/GaSb interlayer (sample # 1041900) cross fringes are observed throughout.

Finally Fig. 21a shows the cross sectional TEM micrograph at the interface of reference sample GaAs/AlSb/GaSb (#5020900). The specimen is rotated about the [110] so a projection of the interface can be seen. The diffraction vector is along the interface (i.e., the same as the axis of rotation), so the contrast in the interface is misfit dislocations that are pointing out towards the viewer. They are spaced at ~50 Å. This corresponds to about 10^{10} misfit dislocation/cm^2. No delineation between the AlSb and GaSb was indicative, indicative of excellent quality of the grown epilayers. The dislocation density decreases with thickness of the film. Some unusual striations were observed in the layer, which were not due to the moiré fringes. They were probably due to the order-disorder transformation caused by compositional modulation. Thin amorphous/ polycrystalline layer was observed on top which we found out later to be due to the presence of Sb flux while cooling the substrate, causing considerable damage to the surface.

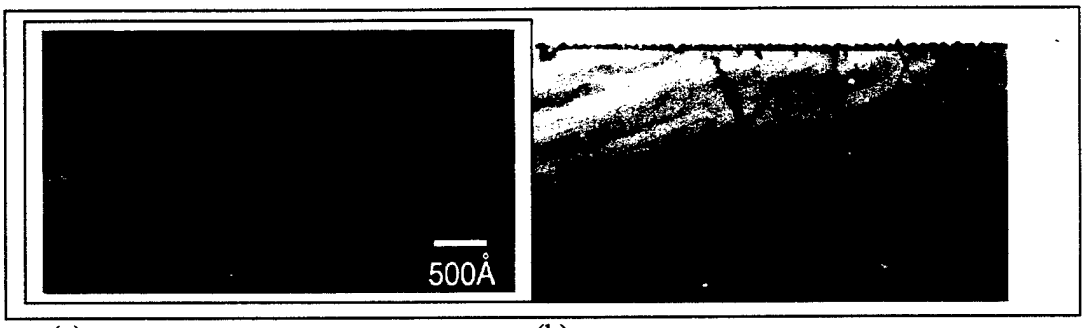

Fig. 21. Cross section TEM micrographs of GaSb grown on AlSb buffer layer (sample # 5020900). In image (a), the specimen is rotated about the [110] direction.

(d) Discussions

The evolutions of the RHEED pattern for all III–Sb on GaAs are similar. The growth becomes rougher (3D) within first few seconds corresponding to probably no more than couple of monolayer before it becomes energetically favorable for 3D clusters of the deposited material's relaxed crystal structure to form. As these clusters grow larger they begin to coalesce leading to the formation of streaks within 10-20". In the case of InSb these have been attributed to the reflection features from In facet planes, which are from (111) and (001)-type facets. After about 15-30" almost continuous streak corresponding to x3 reconstruction pattern is observed as the epilayer dislocates and the surface gets smoother. The growth mode of AlSb on InSb appears to be quite different. It takes longer time to relax and the surface appears to be more diffuse. It is just speculated that probably the activation energy for the growth of III-Sb on III- Sb may be lower leading to high island density. The region between the islands could be the incoherent regions leading to diffuse RHEED lines.

We also found an upper limit to the overlayer growth temperature. For growth temperatures exceeding 500°C resulted in considerable degradation of the surface morphology as observed by Nomarski phase contrast microscope (see Fig.7) and larger x-ray FWHM, typically around 900 arc-secs. This is consistent with RHEED observations shown in Fig.5. The RHEED intensity rapidly decreases beyond 470°C and almost vanishes at 500°C (see Fig.5). These observations suggest dissolution of GaSb at the interface thereby forming the ternary InGaSb, as the melting point of the ternary is very close to that of InSb over a large compositional range. The crystal quality of the layer improves with thickness of GaSb overlayer up to 1.7μm beyond which there is no significant improvement largely as the dislocations have already dispersed.

The thickness of the InSb interlayer appears to influence the crystal quality of the GaSb overlayer. GaSb layer grown on InSb thickness of 36 Å, is very defective as indicated by AFM (Fig.6) and TEM images (Fig 15). The layers grown on thicker InSb epilayer of 120 Å exhibited mosaic tilts, as evidenced from reciprocal lattice mapping measurements (Fig. 14b) while the one with 230 Å did not exhibit any such tilts (Fig. 14a) with the lowest x-ray FWHM of 600 arc-sec.

As GaSb epilayer grown on AlSb buffer layer improves the surface morphology and the crystal quality of GaSb, and also as the ternary InAlSb melting point changes significantly with even small a/o of AlSb, use of a different strained layer namely AlSb in place of GaSb was attempted, to minimize the problem of dissolution of GaSb interlayer at growth temperature of 500^0C normally used for GaSb overlayer growth. However, the surface morphology for these layers indicate that the morphology is dominated by the stacking faults (Fig. 10) while the one with GaSb interlayer (Fig. 9) are dominated by hillocks or growth steps with significantly less dislocation density. Though the overlayer growth temperature can be increased to as much as 510^o C before any RHEED deterioration is observed, the immiscibility of the AlSb with InSb probably allows the propagation of these stacking faults into the GaSb overlayer. Due to the low melting point of (In,Ga)Sb at the growth temperature, the layer may become soft and accommodates the strain by generation of large misfit dislocations at the GaAs/InSb interface, which may impede the motion of stacking faults.

TEM micrograph clearly indicates that the dislocations generated at the interface do not propagate beyond 200 nm inside GaSb overlayer. The dislocations are considerably reduced and the quality of the GaSb layer is of excellent quality as evidenced by the cross fringes observed in the high resolution TEM in the entire region examined and bright spotty crystalline diffraction pattern. This is also consistent with the very bright RHEED pattern that is obtained on these layers in comparison to the ones obtained when GaSb is directly grown on GaAs. So the large value of FWHM of x-ray is thus somewhat misleading and arises probably due to the fact that x-ray beam probes the interfacial region also leading to broadening of the spectra. It is highly probable that if one grows ten micron thick layer the quality of the layer will be much improved over the layers grown directly on GaAs.

(e) Conclusions

In this work we have successfully demonstrated the use of a low temperature interlayer to reduce the threading dislocation density in the mismatched overlayer. Amongst the different interlayers examined, InSb/GaSb interlayer appears to be the most promising one. The GaSb overlayer grown on these interlayers exhibits dislocation

density $<10^7/cm^2$ with excellent structural quality as seen by the transmission electron microscope. RHEED pattern observed in these layers are very unique with all principal and one third integer orders equally bright, not observed when GaSb is grown directly on GaAs. This confirms the excellent quality of the layer. Thus this concept can be extended to the growth of any alloy system and definitely superior to all the existing techniques, as the growth of interlayers is a part of the growth process and do not require a separate processing step.

(f) Bibliography

1. R.Beanland, D.J.Goodhew, *Advances in Physics*, 45(2), 87-146 (1996).
2. D.Teng and Y.H. Lo, *Appl. Phys.Lett.*, 62(1), 43 (1993).
3. P Chavarkar, S.Mathis, L.Zhao, S. Keller, J.S.Speck, and U.K.Mishra, *Jounal of Electronic Material*, 29(7), 944-949 (2000)
4. R.N. Kyutt, R. Scholz, S.S. Ruminov, T.S. Argunova, A.A. Budza, S.V. Ivanov, P.S. Kop"ev, L.M. Sorokin and M.P. Shcheglov, *Phys. Solid Stae* 35, 372 (1993).
5. A. E. Romanov, and J. S. Speck, *Journal of Electronic Materials*, Vol. 29, No. 7,901(2000).
6. S.J. Brown, M.P. Grimshaw, D.A. Ritchie and G.A.C. Jones, *Appl. Phys. Lett.* 69, 1468 (1996).
7. B. Brar and D.Leonard, *Appl. Phys. Lett.* 66, 463 (1995).
8. S.V.Ivanov, A.A.Boudza, R.N.Kutt, N.N.Ledentsov, B.Ya.Meltser, S.S.Ruvimov, S.V.Shaposhnikov, P.S.Kop'ev . *Journal of Crystal Growth* 156, 191-205(1995).

B. Electronic Properties of Heteroepitaxial Undoped and n-InSb Epilayers Using SnTe Source by Molecular Beam Epitaxy

JOURNAL OF APPLIED PHYSICS VOLUME 91, NUMBER 12 15 JUNE 2002

Electronic properties of heteroepitaxial undoped and *n*-InSb epilayers using SnTe source by molecular beam epitaxy

T. A. Rawdanowicz[a)] and S. Iyer[b)]
Department of Electrical Engineering, North Carolina A&T State University, Greensboro, North Carolina 27411

W. C. Mitchel, A. Saxler, and S. Elhamri
Air Force Research Laboratory, Materials and Manufacturing Directorate, AFRL/MLPS, Wright-Patterson Air Force Base, Ohio 45433-7707

(Received 27 December 2001; accepted for publication 12 March 2002)

We report on the electrical characteristics of InSb and *n*-type doping of InSb layers grown on GaAs substrates using a SnTe captive source by molecular beam epitaxy (MBE). The undoped epilayers are *n*-type in the temperature range of 10 to 300 K investigated. Doped layer with carrier concentrations ranging from $2\times10^{16}/cm^3$ to $3.2\times10^{18}/cm^3$ with corresponding x-ray full width at half maxima varying from 170–200 arcsec have been achieved. High carrier mobility of 94 098 cm^2/V s on lightly doped samples has been achieved. These results suggest SnTe source as being one of the donor dopants of choice for MBE grown InSb epilayers. Temperature and magnetic field dependent Hall and resistivity measurements with various multicarrier conduction analysis techniques indicate three conduction channels for undoped InSb and two conduction channels for doped InSb. They have been used successfully to explain the temperature and thickness dependence of the electrical properties of MBE grown undoped and doped InSb epilayers. © *2002 American Institute of Physics*. [DOI: 10.1063/1.1476086]

I. INTRODUCTION

The thin layers of InSb and InSb-based alloys have found considerable interest because of potential applications in groups III–V semiconductor-based infrared optoelectronic devices.[1] The small effective mass and consequent high mobility of the carriers have been utilized in the fabrication of high frequency and high-speed circuit devices,[2] and magnetic field sensors.[3] From a technology point of view heteroepitaxy of InSb on GaAs substrates is advantageous for monolithic integration of InSb devices on GaAs substrates in microelectronics and infrared detector array fabrication. Hence, InSb growth on GaAs has been the subject of extensive study. It has been well demonstrated that the characteristics of the InSb epitaxial layers, particularly at low temperatures, exhibit the deleterious effect of the lattice mismatch between the substrate and the epitaxial layer. Hence, electrical assessment of these narrow bandgap epilayers poses a challenge due to the lack of a suitable lattice matched semi-insulating substrate.

N-type doping of these Sb based compounds, namely, InSb and GaSb has commonly been accomplished using either group IV elements such as Si or Sn, or with the group VI elements, namely, S, Se, or Te. Of the group VI elements, Te is the most suitable dopant due to its relatively low vapor pressure. However, the vapor pressure is high enough to cause sufficient memory effect during MBE growth. Hence different telluride compound sources such as GaTe,[4] PbTe,[5,6] Sb_2Te_3,[7] and SnTe[8] have been investigated as the dopant sources. Among these, GaTe and SnTe were found to be the most effective dopant sources that exhibited excellent control over a concentration range of greater than two orders of magnitude in GaSb. In this work, we have examined SnTe as an *n*-type dopant source for InSb layers. We have also carried out in detail the electrical characterization of these doped epilayers in conjunction with the undoped epilayers grown on GaAs in order to delineate the effect of the interface from the bulk using variable magnetic field measurements with various multicarrier analysis techniques.

II. EXPERIMENTAL DETAILS

The InSb layers were directly grown on semi-insulating GaAs (100) substrates in an EPI 930 system. The sources used were elemental In (7N), Sb (6N5), and compound source SnTe (5N) for dopant. The cracking zone temperature of 950 °C was used for the Sb cracker cell to obtain Sb_2 species. The layers were grown at a growth temperature of 400 °C at 1 μm/h with a beam equivalent pressure ratio of Sb_2/Ga about 2, an optimal growth condition found for the InSb layer in our system. For the growth of the doped InSb layer, the operation cell temperature range was between 275–390 °C.

Reflection high energy electron diffraction (RHEED) was used to monitor the *in situ* growth of the epilayer. During the deposition of the first monolayer (ML) of InSb, the RHEED pattern remained essentially unchanged, the same as that of GaAs (2×4) pattern. After about 1–2 ML of InSb growth, dots in the hexagonal pattern appear, indicative of 3-dimensional nucleation, due to the large lattice mismatch

a)Present address: Department of Materials Science and Engineering, North Carolina State University, Raleigh, NC 27695.
b)Electronic mail: iyer@ncat.edu

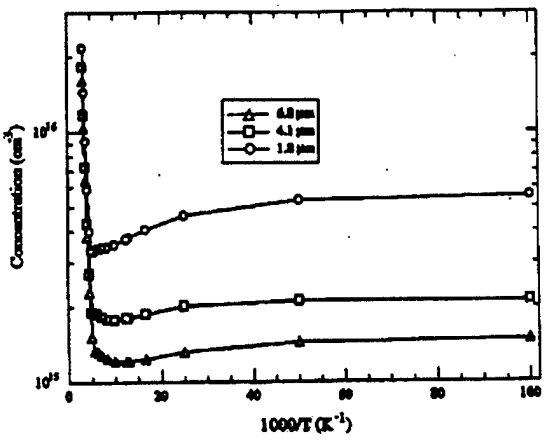

FIG. 1. Hall concentration as a function of reciprocal temperature for undoped InSb samples 523, 709, and 1029 of different epilayer thickness.

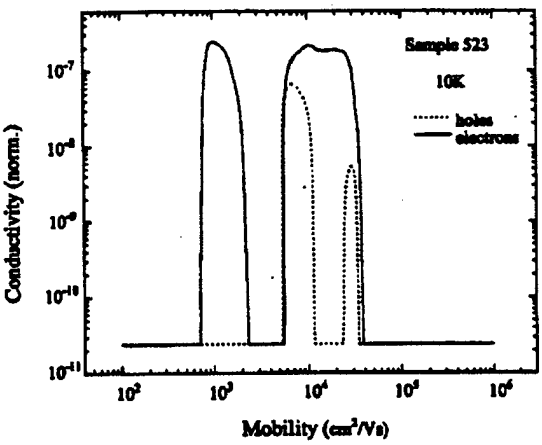

FIG. 3. QMS results for the 4.1 μm undoped InSb sample at 10 K.

(14.6%) between the layer and the substrate. The RHEED spotty pattern develops into a continuous (1×3) streaky reconstruction after about growth of ~~20 ML~~, as the epilayer relaxes upon formation of dislocations and appears to become smooth, having very little intensity modulation as the growth proceeds.

For electrical transport measurements, the wafers were cut into 6 mm squares. A cloverleaf pattern was etched on the epilayer for van der Pauw measurements. Indium metal contacts were made directly on the epilayer by pressure. Temperature dependent Hall effect and resistivity measurements were made in either a closed cycle helium refrigerator or a helium vapor cryostat. Standard single magnetic field Hall effect and resistivity measurements were made from 10 to 300 K. In addition, magnetic field dependent measurements were made at several temperature points in this temperature range at fields up to 2 T. The data were analyzed with three different techniques: conventional mobility spectrum,[9] quantitative mobility spectrum (QMS) analysis,[10] and the multicarrier analysis technique of Kim *et al.*[11] High resolution x-ray diffraction was used to assess the structural quality of the layers.

III. RESULTS

A. Undoped InSb/GaAs

Unintentionally doped InSb on GaAs layers were grown to confirm the quality of the growth process. The full width half maxima (FWHM) of (400) x-ray rocking curve ranged between 98 to 160 arcsec for 4–5-μm-thick InSb layers attesting to the good quality of the layers grown. Figure 1 illustrates the measured Hall concentrations versus inverse temperature for three undoped InSb layers of different thicknesses, while the Hall mobility versus temperature data are shown in Fig. 2. All the layers were *n*-type throughout the entire temperature range investigated. Intrinsic conduction dominated at high temperatures, but the measured concentration varied as a function of thickness at low temperatures.

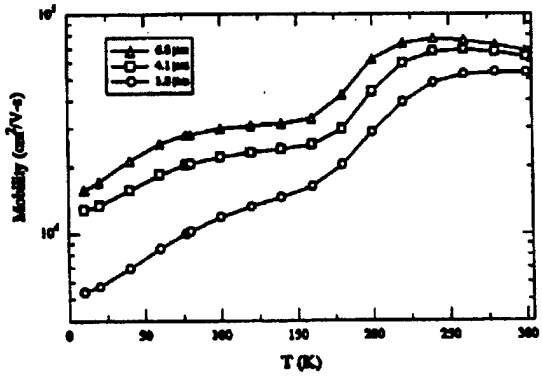

FIG. 2. Hall mobility as a function of temperature for undoped InSb/GaAs samples 523, 709, and 1029 of different epilayer thickness.

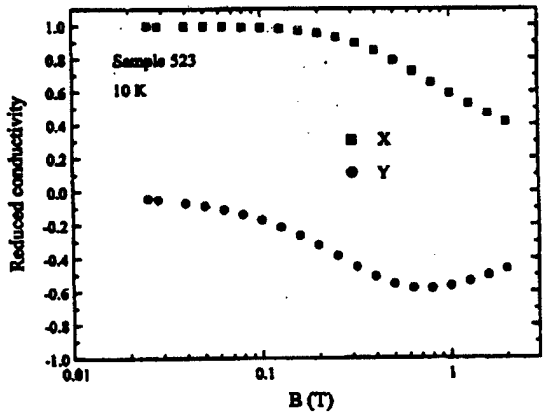

FIG. 4. Reduced conductivities from KST analysis as a function of magnetic field for the 4.1-μm-thick undoped InSb sample at 10 K.

TABLE I. Results of KST analysis of InSb on GaAs, areal concentrations and mobilities for each of three conduction channels for undoped samples 602 and 523 and *n*-type SnTe doped sample 715.

T (K)	$n_1\times10^{11}$ (cm^{-2})	μ_1 (cm^2/Vs)	$n_2\times10^{11}$ (cm^{-2})	μ_2 (cm^2/Vs)	$n_3\times10^{11}$ (cm^{-2})	μ_3 (cm^2/Vs)
No. 602, 4.8 μm						
10	7.85	2933	5.29	5354	5.43	14 150
80	8.1	2800	3.5	9800	2.2	24 000
150	5.6	2900	2.8	8900	3.1	30 000
300			7.4	1870	87	62 000
No. 523, 4.1 μm						
10			14	2600	5.8	14 000
200			15	6700	12	49 000
300	58	480	41	16000	54	62 000
No. 715, 5.8 μm						
10			11	4700	44	41 000
100			12	2100	33	47 000
200			8.4	2553	39	41 000
300			8.4	2553	35	36 000

where the temperature dependence was very weak. The lowest measured concentration, 1.3×10^{15} cm^{-3}, was for the thickest sample, but even the highest concentration, 5.5×10^{15} cm^{-3}, was relatively low. As seen in Fig. 2, the thickest sample has the highest mobility throughout the whole temperature range.

Thickness dependent concentrations and mobilities often suggest the presence of more than one conduction channel. Magnetic field dependent measurements were made at several temperatures for two of the undoped samples and analyzed with three multicarrier techniques; standard mobility spectrum,[9] quantitative mobility spectrum (QMS),[10] and the multicarrier analysis technique of Kim *et al.* (KST).[11] The QMS and KST results for the 4.1-μm-thick sample at 10 K are shown in Figs. 3 and 4, respectively. Figure 3 shows the conductivity as a function of mobility as determined from the QMS analysis, while Fig. 4 depicts the longitudinal (X) and transverse (Y) components of the reduced conductivity tensor from the KST analysis of $R_{xx}(H)$ and $R_{xy}(H)$ for sample 523. The quantitative results of the KST analysis for the two undoped samples and one *n*-type doped sample are given in Table I. The 4.8-μm-thick sample, No. 602, shows three conduction paths at lower temperatures, but only two at room temperature. The 4.1 μm sample, No. 523, shows only two conduction paths at low temperatures and possibly three at room temperature.

B. Doped InSb

The thickness of all the doped samples grown were close to 5.7 μm to minimize the effect of the thickness dependence. The FWHM of (400) x-ray rocking curve varied from 170 to 200 arcsec corresponding to the carrier concentrations variation from $2\times10^{16}/cm^3$ to $3.2\times10^{18}/cm^3$.

Figure 5 shows the measured Hall concentration versus inverse temperature curves for samples grown with different SnTe source temperatures. The absence of temperature dependence indicates the presence of impurity banding due to heavy doping. Conductivity is dominated by electrons, but the electron mobility is reduced by impurity scattering. This is also seen in the mobility versus temperature results shown in Fig. 6. Only in the sample with the least amount of dopant is there significant temperature dependence to the mobility, reaching as high as 94 098 cm^2/V s at 77 K.

The room temperature and 77 K mobilities as a function of carrier concentration for both the doped and undoped samples are shown in Figs. 7 and 8, respectively. The room temperature results follow the expected behavior, but the 77 K results are anomalous in that the mobilities for the undoped samples are actually lower than for many doped samples with higher concentrations.

An Arrhenius plot of the doping Hall concentration as a function of the reciprocal of the SnTe source temperature is shown in Fig. 9. The solid line represents the vapor pressure of SnTe with the literature value (1.99+/−0.11 eV) for the enthalpy of sublimation. The actual activation energy is within experimental error of the literature value so that the doping level may be considered proportional to the arrival rate of the molecular species up to about 3×10^{18} cm^{-3}.

Magnetic field dependent measurements were made on one doped sample, No. 715, with a dopant source tempera-

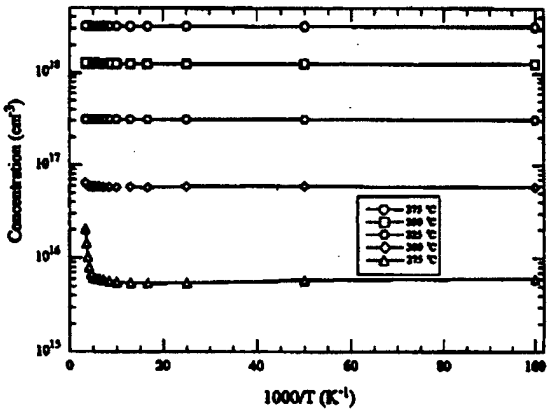

FIG. 5. Hall concentrations as a function of reciprocal temperature for doped InSb/GaAs samples 715, 716, 717, 723, and 725 of different SnTe dopant temperatures.

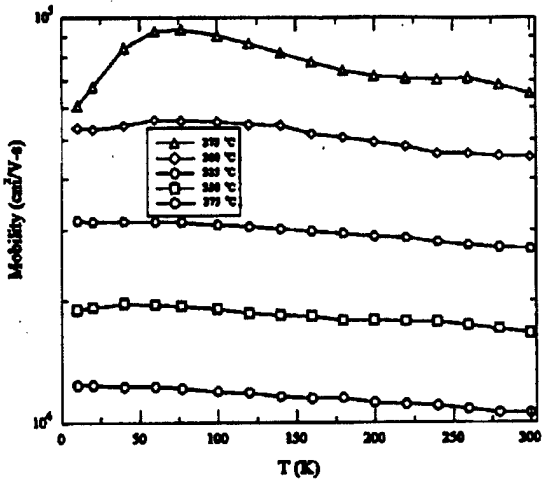

FIG. 6. Hall mobility as a function of temperature for undoped InSb/GaAs samples 715, 716, 717, 723, and 725 different SnTe dopant temperatures.

ture of 300 °C. The mobility spectrum of the doped sample, No. 715, showed only two peaks, one attributed to the bulk and the other ~~one~~ attributed to the interfacial layer. The QMS results at room temperature are shown in Fig. 10. The results of the KST analysis on this sample at four temperatures are given in Table I.

IV. DISCUSSION

Both surface accumulation layers[12,13] and conducting interface layers[14,15] have been reported in InSb grown on GaAs. Our multicarrier analysis suggests the presence of three channels in our InSb on GaAs samples. In addition, at higher temperatures intrinsic conduction complicates the analysis of transport data. The intrinsic mobilities of electrons and holes in InSb at 300 K are 80 000 and 1 250 $cm^2/V\,s$, respectively.[16] The 2 T magnetic field limit on our magnet prevents us from reliably identifying conduction channels with mobilities less than 2 000 $cm^2/V\,s$ with any of

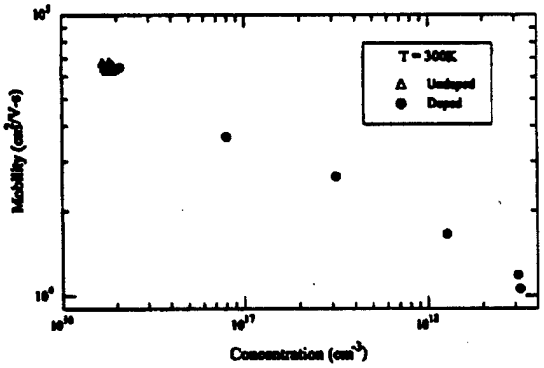

FIG. 7. Hall mobility vs the Hall concentration at $T = 300$ K for all undoped and doped InSb/GaAs samples ~~except 1029 and 1030.~~

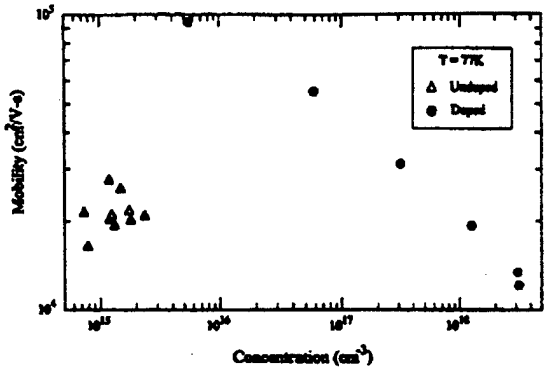

FIG. 8. Hall mobility vs the Hall concentrations at $T = 77$ K for all undoped and the doped InSb/GaAs samples ~~except 1029 and 1030.~~

the three multicarrier analysis techniques, so we were unable to observe the intrinsic holes at room temperature. This makes the quantitative results at this temperature somewhat suspect. However, the magnetic field dependent data and the multicarrier analysis results demonstrate that there are at least two and sometimes three electron conduction channels in our samples. Following the literature, we attribute these to bulklike conduction, a surface accumulation layer, and possibly an interface layer between the GaAs substrate and the InSb. The interface layer will have the poorest crystalline quality of the three channels due to misfit dislocations.[17] Therefore, we assume that the mobility in this channel will be the lowest, corresponding to mobility μ_1 of Table I. The interface layer is not observed in all samples because the mobility is below our detection limit with multicarrier analysis. The surface accumulation layer will also have a lower mobility than the bulk due to surface states and heavier electron effective mass. The Hall concentration in this layer will have a low to negligible temperature dependence because the concentration depends on band bending and not on thermal activation. We attribute the Hall concentration n_2 and mobility μ_2 in Table I to a surface accumulation layer. The carrier concentration in the bulklike layer will show intrinsic con-

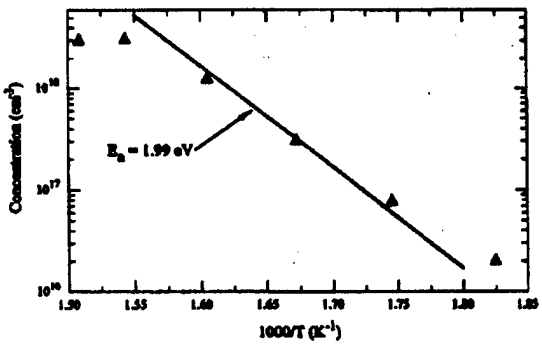

FIG. 9. Room temperature Hall concentration as a function of reciprocal SnTe dopant temperatures for InSb/GaAs. The solid line represents the vapor pressure of SnTe calculated based on its enthalpy of sublimation (1.99 eV).

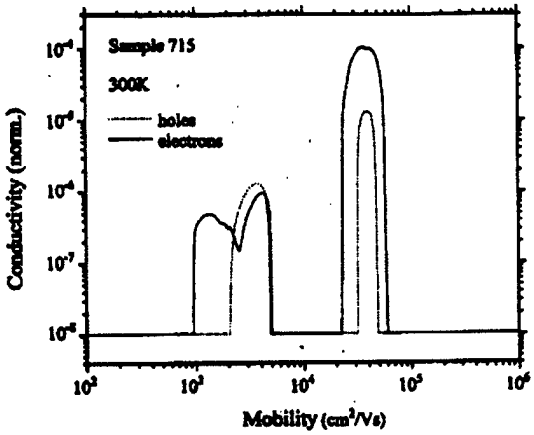

FIG. 10. QMS results for doped InSb sample No. 715 at room temperature.

duction at high temperatures and then become relatively independent of temperature due to the very shallow nature of donors in InSb [0.67 meV (Ref. 18)]. Although shallow donors will be ionized even at 10 K, the temperature dependence of the carrier concentration will be determined by factors such as the deep level donors and/or possibly shallow acceptors due to the electrically active dangling bonds at the highly mismatched interface.[19]

The fact that the apparent low temperature electron concentration varies with sample thickness (Fig. 1) for the undoped samples can be explained by invoking the multichannel conduction process. The areal density of carriers in the surface accumulation and interface layers does not depend on thickness of the sample, however the areal density of the carriers in the bulklike layer will vary with thickness, as the residual donor and acceptor volume concentrations are independent of thickness. For thin samples, the surface and interface layers will dominate, but the bulklike layer will dominate for thicker samples. Similar effects will occur for the mobility.

The surface and interface layers will not be as influential in the doped samples because of the higher concentration of carriers in the bulklike layer compared to the surface and interface layers. The additional carriers will satisfy the dangling bonds at the interface. In addition, the band bending is larger and deeper for the undoped materials that extend significantly into the layer. The influence of the surface states will be minimized when the compensation is reduced or eliminated. Hence, at sufficiently high doping concentration, the bulklike layer will completely dominate even in the thinnest samples. As can be seen in Table I, at no temperature is the concentration of the bulklike layer in the doped sample less than a factor of 3 above that in the surface layer, while in the undoped samples at low temperatures the areal concentrations of both the surface and the interface layers equal or exceed the areal concentration in the bulklike layer.

The fact that the mobilities of the undoped samples at 77 K are lower than the mobilities of the lowest concentration doped samples presently cannot be explained by the multicarrier analysis. Examination of Table I indicates the mobility μ_3 of the bulk layers in the two undoped samples at temperatures below 200 K are lower than that of the doped sample even though the electron concentration n_3 in the bulklike layer of the doped sample is higher at these temperatures than those in the bulklike layers of the undoped samples.

Sn can be amphoteric in group III–V semiconductors depending on the sublattice that it occupies, being a donor when on the group III lattice and an acceptor when on the group V lattice. Since the covalent radii of Sn (1.40 Å) is comparable to both In (1.44 Å) and Sb (1.36 Å), the question arises whether or not a group IV element will occupy both sublattices in group III–V materials, like Ge in GaAs, which produces both donors and acceptors at the same time, resulting in low mobility, heavily compensated material. The fact that the low temperature mobilities for the lightly doped InSb samples in this study are higher than the undoped samples suggest that compensation is not a major problem in the doped samples. This indicates that the doping does not produce extra acceptors, as it would if Sn went in on both sublattices. Te will be a donor regardless of the sublattice.

The Hall mobility values obtained on these samples are in excellent agreement with the values reported[5] on PbTe doped InSb over the entire concentration range. Further, the FWHM of (400) x-ray rocking curve are narrow exhibiting a weak dependence with concentration varying from 170 to 200 arcsec with carrier concentration increase from 2×10^{16} cm^{-3} to 3.2×10^{18} cm^{-3}. This attests to the good structural quality of the doped epilayers. This is in contrast to the much larger increase in x-ray rocking curve width reported for Si doped InSb,[20] while there are no reports on PbTe doped InSb.

In conclusion, the temperature and magnetic field dependent variations of the Hall effect and resistivity measurements in conjunction with multicarrier analysis in MBE grown undoped InSb heteroepilayers indicate the presence of three conduction channels attributed to the high mobility bulklike, interfacial, and a surface layer. The variation in the carrier concentration and mobility with temperature and thickness has been explained using the multichannel conduction process. We have also successfully grown p/N-type non-amphoteric SnTe doped InSb epilayers. The results suggest SnTe is a well-behaved *n*-type dopant without any significant compensation in MBE grown InSb epilayers. The carrier concentration could be varied over two orders of magnitude and covers the range of interest for device applications. Multicarrier analysis in the doped InSb indicates the presence of only two conduction channels due to the bulklike layer and surface layer.

ACKNOWLEDGMENTS

This work was supported by Air Force Office of Scientific Research (AFOSR): Grant Nos. F49620-95-1-05 and F49620-98-1-0328. The authors thank Jie Li for technical assistance.

[1]E. Michel, G. Singh, S. Slivken, C. Besikci, P. Bove, I. Ferguson, and M. Razeghi, Appl. Phys. Lett. 65, 3338 (1994).

[3]T. Ohashi, D. P. Bour, T. Itoh, J. D. Berry, S. R. Jost, G. W. Wicks, and L. F. Eastman, J. Vac. Sci. Technol. B 4, 622 (1986).
[5]J. Heremans, J. Phys. D 26, 1149 (1993).
[4]G. W. Turner, S. J. Eglash, and A. J. Strauss, J. Vac. Sci. Technol. B 11, 864 (1993).
[5]D. L. Partin, J. Heremans, and C. M. Thrush, J. Appl. Phys. 71, 2328 (1992); J. Cryst. Growth. 111, 614 (1991).
[6]S. Subbanna, G. Tuttle, and H. Kroemer, J. Electron. Mater. 17, 297 (1988).
[7]T. H. Chiu, J. A. Ditzenberger, H. S. Luftman, W. T. Tsang, and N. T. Ha, Appl. Phys. Lett. 56, 1688 (1990).
[8]J. F. Chen and A. Y. Cho, J. Appl. Phys. 70, 277 (1991); J. Electron. Mater. 22, 259 (1993).
[9]W. A. Beck and J. R. Anderson, J. Appl. Phys. 62, 541 (1987).
[10]I. Vurgaftman, J. R. Meyer, C. A. Hoffman, D. Redfern, J. Antoszewski, L. Faraone, and J. R. Lindemuth, J. Appl. Phys. 84, 4966 (1998).
[11]J. S. Kim, D. G. Seiler, and W. F. Tseng, J. Appl. Phys. 73, 8324 (1993).
[12]J. R. Söderström, M. M. Cumming, J.-Y. Yao, and T. G. Andersson, Semicond. Sci. Technol. 7, 337 (1992).
[13]C. Besikci, Y. H. Choi, R. Sudharsanan, and M. Razeghi, J. Appl. Phys. 73, 5009 (1993).
[14]E. Michel, H. Mohseni, J. D. Kim, J. Wojkowski, J. Sandven, J. Xu, M. Razeghi, R. Bredthauer, P. Vu, W. Mitchel, and M. Ahoujja, Appl. Phys. Lett. 71, 1071 (1997).
[15]M. Ahoujja, W. C. Mitchel, E. Michel, and M. Razeghi, in *Semiconducting and Insulating Materials—1998*, edited by Z. Liliental Weber and C. Miner (IEEE, Piscataway, NJ, 1999), pp. 177–180.
[16]S. M. Sze, *Physics of Semiconductor Devices*, 2nd ed. (Wiley, New York, 1981).
[17]X. Weng, R. S. Goldman, D. L. Partin, and J. P. Heremans, J. Appl. Phys. 88, 6276 (2000).
[18]See, for example, Ya. M. Gal'perin, E. M. Gershenzon, I. L. Drichko, and L. B. Litvak-Gorskaya, Fiz. Tekh. Poluprovodn. 24, 3 (1990) [Sov. Phys. Semicond. 24, 1 (1990)].
[19]T. Tanaka, M. Washima, and H. Sakaguchi, Jpn. J. Appl. Phys., Part 1 38, 1107 (1999).
[20]Philip E. Thompson, John L. Davis, Ming-Jey Yang, David S. Simons, and Peter H. Chi, J. Appl. Phys. 74, 6686 (1993).

Seiler

C. Photoreflectance Studies of Te-doped GaSb at the $E_0+\Delta_0$ Transition

Photoreflectance studies of Te-doped GaSb at the $E_0+\Delta_0$ transition

S. Iyer,[a] S. Mulugeta, W. Collis, and S. Venkatraman
Department of Electrical Engineering, North Carolina A & T State University, Greensboro, North Carolina 27411

K. K. Bajaj and G. Coli
Department of Physics, Emory University, Atlanta, Georgia 30322

(Received 17 June 1999; accepted for publication 19 November 1999)

Photoreflectance (PR) response of bulk and epitaxially grown Te-doped GaSb samples at the higher energy $E_0+\Delta_0$ transition has been investigated from 4 K to room temperature. The PR spectra did not exhibit any Franz–Keldysh oscillations and are described using the third derivative of the Lorentzian functional form of the dielectric function. Using line shape analysis of the PR spectra, the temperature dependence of the $E_0+\Delta_0$ transition energy has been obtained. The value of the $E_0+\Delta_0$ transition energy in a bulk grown sample, with an electron concentration of about $1.6\times10^{17}/\text{cm}^3$, is found to be 1.583 eV at 4 K. For more heavily doped epitaxially grown samples with an electron concentration of $7.4\times10^{17}/\text{cm}^3$, the value of $E_0+\Delta_0$ is determined to be 1.613 eV. The contributions of the many-body effects such as band filling and band gap renormalization on the $E_0+\Delta_0$ transition are calculated and are used to explain the measured values. © *2000 American Institute of Physics.* [S0021-8979(00)07505-8]

I. INTRODUCTION

Photoreflectance (PR) is a well known contactless semiconductor characterization technique that allows the determination of the critical-point energies and the evaluation of the quality of the material in an expeditious manner. The dominant mechanism responsible for the PR signal has been attributed to the modulation of the built-in surface electric field by the photogenerated carriers. The application of this technique to narrow band gap III–V semiconductor materials has been somewhat limited[1,2] because of the low values of the built-in electric field. However, Beaulieu *et al.*[1] and Hwang *et al.*[2] have reported PR studies in InSb at 8 K and in undoped GaSb from 83 to 300 K, respectively.

The object of our work is to carry out a PR study on both *n*-type and intentionally undoped GaSb samples. This investigation was carried out at the $E_0+\Delta_0$ transition for the following reasons. The PR signal at the fundamental band gap E_0 is usually obscured by strong luminescence from the sample, particularly at low temperatures. On the other hand, the luminescence is somewhat weaker for higher energy transitions, such as at $E_0+\Delta_0$, and hence, can be reduced considerably by normalization methods. Second, the $E_0+\Delta_0$ transition has an advantage over higher critical points, in that it can be used to investigate the dependence of PR signal on dopant concentration, since both E_0 and the $E_0+\Delta_0$ transitions exhibit the same shift towards higher energy with doping. Third, at this energy (1.5 eV at 300 K) the penetration depth of the probe beam is

$$\alpha^{-1}=\lambda/(4\pi\kappa)=191\ \text{nm},$$

where $\lambda(\sim827\ \text{nm})$ is the wavelength of the probe beam and $\kappa=0.344$ is the extinction coefficient[3] in GaSb at 1.5 eV. The PR signal therefore originates from approximately the top 200 nm of the samples, and hence, allows the investigation of relatively thin films.

II. EXPERIMENTAL DETAILS

A standard PR system was utilized. The probe beam, light from a 100 W quartz-tungsten halogen lamp source dispersed through a 0.25 m monochromator, is focused on an area of 2 mm^2 on the sample. Photomodulation was achieved by a He–Ne laser operating at 632.8 nm and chopped at 250 Hz. A silicon photodiode was used as a detector to measure both the dc and the ac components of the signal. Spurious ac background signals due to photoluminescence and pump beam scattering are minimized by placing two optical filters in front of the detector. Any spurious ac background remaining after optical filtering is subtracted by zeroing the lock-in amplifier (adjusting the offset) with the probe beam off.

Samples used in this study are bulk grown GaSb provided by Metal Specialities and epitaxial layers of GaSb grown on the conducting (100) GaSb substrates by liquid phase electro-epitaxy (LPEE) and by molecular beam epitaxy (MBE) in our laboratory. The LPEE and MBE layers were grown at a temperature of 476 and 530 °C, respectively. These samples were doped with elemental Te and SnTe sources, respectively. Three samples, one bulk and one each from the LPEE and MBE groups referred to as sample B, L, and M, respectively, were chosen for detailed PR investigations. The epitaxial layers were approximately 2 and 4 μm, thick, respectively. The full width at half maximum of the x-ray rocking curves of sample B was determined to be 18 arc sec and those of L and M were around 38–40 arc sec, attesting to the good structural quality of our samples.

[a]Electronic mail: iyer@genesis.ncat.edu

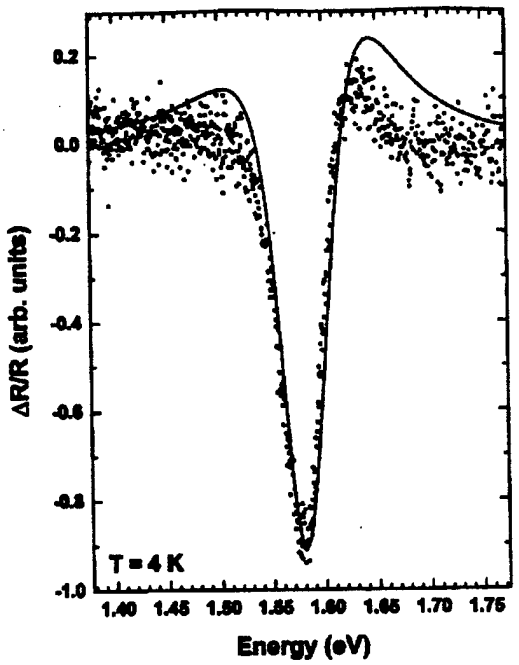

FIG. 1. PR spectrum of bulk Te-doped GaSb sample B at 4 K. The solid line is a least-squares fit to a third derivative functional form.

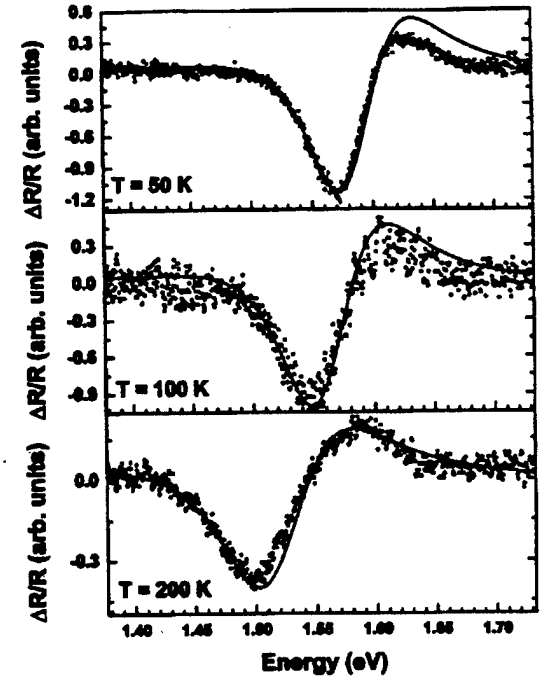

FIG. 2. PR spectra of bulk Te-doped GaSb sample B at 50, 100, and 200 K. The solid lines are least-squares fits to Eq. (1).

III. RESULTS AND DISCUSSION

Figure 1 shows the PR spectrum of Te-doped GaSb sample B at 4 K. The absence of Franz–Keldysh oscillations clearly suggests that we are in the low field regime. The line shape was also found to be independent of the modulating pump intensity in the limited range investigated. Further, as discussed later the line shape is fitted very well using a Lorentzian third derivative functional form. All these observations are signatures of the PR spectra in the low field regime.

The PR spectra were analyzed using the equation[4]

$$\Delta R/R = Re[Ce^{i\theta}(E-E_{cp}+i\Gamma)^{-n}], \tag{1}$$

where $E=\hbar\omega$ represents the energy of the probe beam, C and θ are an amplitude and a phase factor, respectively, that varied slowly with E; E_{cp} and Γ are the critical-point energy and a broadening parameter, respectively, and n refers to the type of the critical point in question. The value of $n=2$ corresponds to an excitonic transition and values of $n=2.5$ and 3 correspond to band-to-band transitions at a three-dimensional (3D) and a two-dimensional critical point, respectively. The best fit was obtained for $n=2.5$, as illustrated in Fig. 1, thus suggesting a band-to-band transition at a 3D critical point. The value of $E_0+\Delta_0$ transition energy, from hereon referred to as E_P, is determined to be 1.585 eV and is somewhat larger than a relatively precise value of 1.571 eV reported in literature[5] for intentionally undoped samples. The reason for this difference will be discussed later in this article.

Figure 2 illustrates the PR spectra of sample B at several higher temperatures. It may be noted that the overall shape of the spectra does not change with temperature. However, the PR spectrum shifts to lower energies and becomes broader as the temperature is increased. The values of E_P at these temperatures are determined by the line shape analysis as described earlier and are plotted as a function of temperature in Fig. 3. The following empirical relation due to Varshni[6] has been used to describe the temperature dependence of the $E_0+\Delta_0$ transition, $E_P(T)$,

$$E_P(T)=E_P(0)-\alpha T^2/(\beta+T), \tag{2}$$

where $E_P(0)$ is the value of E_P at $T=0$ K and α and β are the fitting parameters. The values of α (5.5×10^{-4} eV/K), and β (175±10 K) are found to be somewhat smaller than those of Hwang *et al.*,[2] $6.5(\pm0.2)\times10^{-4}$ eV/K and 230±10 K, respectively.

The PR spectra of epilayers L and M at 4 K are similar in shape to bulk sample B but are considerably broader due to the presence of much larger concentration of impurities and defects. The value of the E_P transition in these two samples is found to be 1.613 eV. We have studied the PR spectra of these two samples up to 250 K. As in the case of sample B, the spectra of these two samples broaden and shift to lower energies with temperature. The values of the fitting parameters α and β are found to be about the same as in sample B.

We now discuss the effects of heavy doping on the value of E_P at 4 K. These effects can be divided into three main categories:

(1) The shape of the density of states of the conduction band is considerably altered by the fluctuations of the electronic potential due to the presence of high concentration of

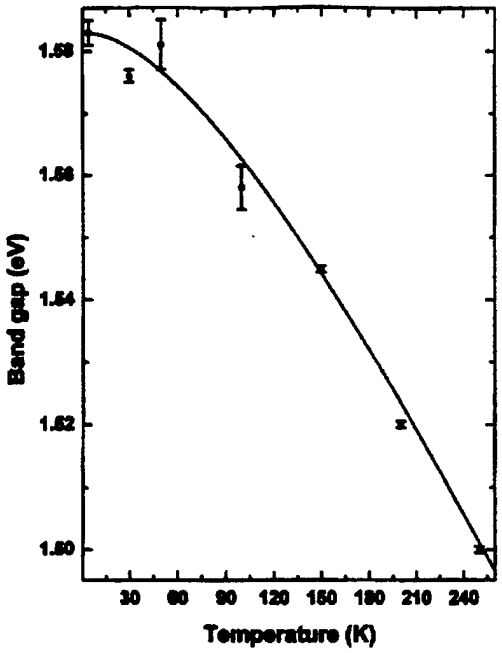

FIG. 3. Temperature dependence of the $E_0+\Delta_0$ transition energy (closed circles). The solid line is a least-squares fit to the Varshni expression of Eq. (2).

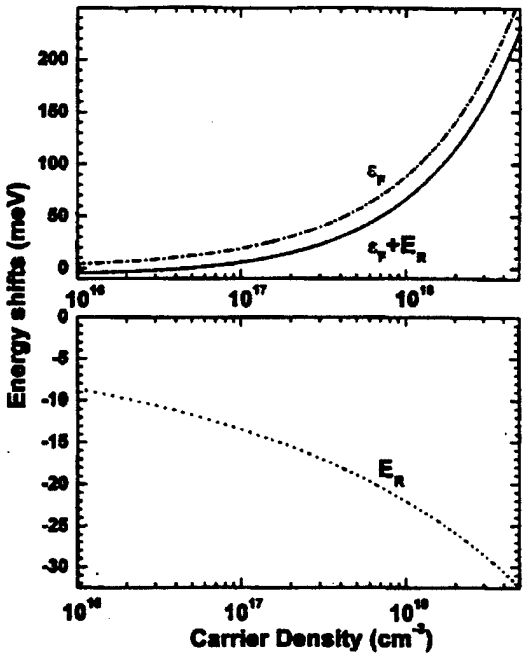

FIG. 4. Fermi energy ϵ_F, band gap renormalization E_R, and total change in the transition energy E_P as a function of carrier concentration are shown, as determined by the formalism in Ref. 7.

ionized impurities and tail states are induced in the energy gap. This has the effect of reducing the value of E_P.

(2) The electron gas at a low temperature is completely degenerate with a well defined Fermi energy. This is the so-called band filling effect which increases the value of E_P.

(3) Many-body effects play an important role in these samples. The correlation effects are rather small but the exchange interactions reduce considerably the value of E_P (band gap renormalization effect).

We have calculated the effects of band filling and band gap renormalization in our samples at 4 K using the formation described in Ref. 7. Figure 4 illustrates the variation of the Fermi energy ϵ_F (dotted line), band gap renormalization energy, E_R and the total change in the value of E_P, ΔE as a function of electron concentration N. At low values of N the magnitude of E_R is somewhat larger than that of ϵ_F. However, for values of N larger than $5\times10^{16}/\text{cm}^3$, ϵ_F becomes more dominant and the value of E_P increases as a function of N. In our sample B the value of N as determined by Hall measurement is about $1.6\times10^{17}/\text{cm}^3$, which corresponds to a value of ΔE of about 11 meV. If we assume that the value of E_P in undoped samples is 1.571 eV,[5] the value of E_P we calculate in our sample is 1.582 eV which is smaller than our measured value of 1.585 eV by 3 meV. Aspnes *et al.*[8] have measured the value of E_P using electroreflectance in GaSb with electron concentration of $1.1\times10^{17}/\text{cm}^3$ and find it to be 1.575 eV, smaller than our value as expected but also smaller than the value we calculate for their electron concentration, by about 3 meV. In epitaxially grown samples L and M we are not able to measure the values of N as these are grown on conducting substrates. The value of E_P we measure in these samples is 1.613 eV which is 42 meV higher than its value in undoped samples. This enhancement in the value of E_P, according to our calculations, corresponds to an electron concentration of about $5.8\times10^{17}/\text{cm}^3$. However, in a GaSb sample grown on a semi-insulating GaAs substrate by MBE under growth conditions nominally identical to those used for the sample M, the electron concentration was measured to be $7.4\times10^{17}/\text{cm}^3$. The calculated value of $E_0+\Delta_0$ transition energy for this electron concentration is found to be 1.62 eV which is larger than the measured value by 7 meV.

As noted earlier, the effect of the tail states is to reduce the value of E_P. Our measured values of E_P contain the contribution of this effect. We therefore suggest that the electron concentration in our samples, as well as in samples studied by Aspnes *et al.*,[8] may be somewhat different than the values used here. In view of some uncertainty in measuring the values of N, this is not unlikely. It should be mentioned that Aspnes *et al.*[8] do not include the band gap renormalization effect in the analysis of their data.

We have estimated the error in the determination of the values of E_P at 4 K using our Lorentzian fitting analysis to be about ($\pm$)3 meV. The error is somewhat larger at higher temperatures. In addition there is about 10% uncertainty in the determination of electron concentration in our samples using Hall measurements. This leads to, for the range of electron concentration in our samples, about 2 meV uncertainty in the value of the energy contribution due to many-body effects. In view of these uncertainties in the values of E_P, the agreement between theory and experiment is very good.

PR signals were not observed in intentionally undoped GaSb samples, which are generally assumed to be p type even at low temperatures. Numerous samples of bulk undoped GaSb and epilayers were examined to confirm this observation. This result is in disagreement with that of Hwang *et al.*[2]

As mentioned earlier, we have been able to fit consistently the observed PR spectra in our samples using the third derivative of Lorentzian form which is appropriate for the band-to-band transition at $E_0+\Delta_0$ critical point. The absence of Franz–Keldysh oscillations, the logarithmic dependence of the PR amplitude on modulation intensity, and invariance of PR line shape with modulating beam intensity, clearly indicate that the dominant mechanism giving rise to PR signal is the modulation of surface space charge field in the low-electric field regime. The width of the depletion region in our samples ranges from 60 to 37 nm at 4 K which is considerably smaller than the penetration depth of the pump beam. As the temperature is increased the spectra become broadened primarily due to the spread of the electron Fermi–Dirac distribution function. The penetration depth has a very weak dependence on temperature[9] and does not significantly affect the modulating field.

The pump beam generates electrons and holes in the depletion region as well as in the rest of the sample. The holes in the depletion region travel towards the surface and neutralize a certain density of surface states responsible for pinning the Fermi level. This effect depends on the intensity of the pump beam. The built-in electric field is reduced and reaches a steady state value which depends on the intensity of the pump beam. We believe that the intensity of the pump beam used in our studies is not large enough to cause flat-band condition. The modulating beam is therefore able to modulate the built-in-electric field to produce a PR signal.

IV. CONCLUSIONS

In conclusion, a detailed study of the $E_0+\Delta_0$ transition energy in Te-doped GaSb epilayers has been made as a function of temperature. The absence of the PR signal from our undoped GaSb samples indicates the presence of a large density of surface states in these samples, pinning the Fermi level close to the valence band. The consistent fit to the third derivative Lorentzian functional form of the PR line shapes suggests band to band transition at a 3D critical point. The dependence of $E_0+\Delta_0$ transition energy on doping levels has been analyzed by including the effects of band filling, band gap renormalization, and tail states. Inclusion of these effects provides a satisfactory explanation of the observed spectra.

ACKNOWLEDGMENTS

This work has been supported by the Air Force Office of Scientific Research (AFOSR) Grant Nos. F49620-98-1-0328 and F49620-95-1-05. The authors would also like to thank P. M. Amirtharaj of NIST, Maryland for critical discussions during the initial experimental setup.

[1] Y. Beaulieu, J. B. Webb, and J. L. Brebner, Solid State Commun. **90**, 683 (1994).
[2] J. S. Hwang, S. L. Tyan, M. J. Lin, and Y. K. Su, Solid State Commun. **80**, 891 (1991).
[3] D. E. Aspnes and A. A. Studna, Phys. Rev. B **27**, 985 (1983).
[4] D. E. Aspnes, Surf. Sci. **37**, 418 (1973).
[5] C. Alibert, A. Joullie, A. M. Joullie, and C. Ance, Phys. Rev. B **27**, 4946 (1983).
[6] Y. P. Varshni, Physica (Utrecht) **34**, 149 (1967).
[7] C. Ell, R. Blank, S. Benner, and H. Haug, J. Opt. Soc. Am. **6**, 2006 (1989).
[8] D. E. Aspnes, C. G. Olson, and D. W. Lynch, Phys. Rev. B **14**, 4450 (1976).
[9] D. C. Look, *Electrical Characterization of GaAs Materials and Devices* (Wiley, New York, 1989), p. 46.

D. UCSB Final Report

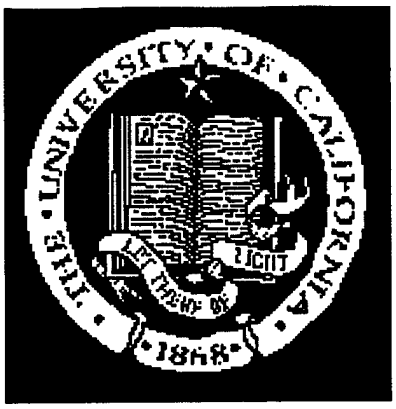

Final Report to

North Carolina A&T

Award Number:
North Carolina A&T #4-41149-S-001
Technical POC: Prof. Shanthi Iyer

PI:
James S. Speck

Materials Department
University of California
Santa Barbara, CA 93106

Objective and Background:
This program involved the development of methods to produce novel routes to high quality lattice mismatched epitaxial layers. At UCSB under earlier AFOSR support, we have developed a new process for producing relaxed buffer layers for subsequent device growth. We refer to these buffers as lattice engineered substrates (LES). In the LES method, a selectively oxidizable layer, such as AlAs, is placed between a lower relaxed layer (*e.g.*, a homoepitaxial buffer layer on a substrate) and a top strained layer. After growth, the epitaxial structure is processed to form either free mesas or stripe mesas. Then the structure is subjected to steam oxidation. We have previously shown that for InGaAs/AlAs/GaAs structures, the conversion of the AlAs to AlO_x is accompanied by strain relaxation and reactive removal of misfit dislocations [Mathis *et al.*, *Appl. Phys. Lett.* **77**, 845 (2000)]. In this program, we studied the lateral oxidation of Ga(As,Sb)/Al(As,Sb)/InP. This work was motivated by the drive to produce high quality buffer layers with lattice constants greater than 6 Å.

Program Activities:

- Comprehensive study of the lateral oxidation of Ga(As,Sb)/Al(As,Sb)/InP
  - Determination of rate limiting processes
    - Low oxidation temperatures: (T_{ox} < 400 °C): reaction limited oxidation
    - Higher temperatures (T_{ox} > 400 °C): diffusion limited or self-limiting
  - Evaluation of the Sb float layer in oxidized structures
    - Morphology
    - Location (toward free surface)

- Evaluation of GaSb layers grown on GaAs with different interlayers at NC A&T
  - Cross-section and plan view TEM studies
  - High resolution x-ray diffraction studies
  - RHEED data interpretation and discussion

Summary of Results on Al(As,Sb) Oxidation:

The lateral oxidation kinetics of $AlAs_{0.56}Sb_{0.44}$ on InP substrates were investigated to understand the antimony segregation process during oxidation. Oxidation layers were grown between GaAsSb buffer and cap layers on InP substrates by molecular beam epitaxy. Oxidation temperatures between 325 and 500 °C were investigated for AlAsSb layer thicknesses between 100 and 2000 Å. At low oxidation temperatures (T_{ox} < 400 °C), the process is reaction limited with a linear dependence of oxidation depth on time. At intermediate oxidation temperatures (400,T_{ox} ,450 °C), the oxidation process becomes diffusion limited. At high oxidation temperatures, the oxidation process is termed self-limiting since at 500 °C the process stops entirely after oxidation times on the order of 5 min and distances of 40 mm. It is shown that the antimony float layer lags the oxidation front by a temperature-dependent distance, which suggests that the antimony may change

the structure of the oxide at the front and cause self-limiting behavior. The oxidation kinetics of $Al_xGa_{1-x}AsSb$ and $Al_xIn_{1-x}AsSb$ have also been investigated. Antimony segregation is not suppressed during oxidation of Ga-containing layers and AlInAsSb quaternary alloys do not oxidize laterally at measurable rates in the range 400–525 °C. SiN_x cap layers deposited after growth and before oxidation do not affect the Sb segregation or oxidation rate, but do smooth the cap surface by preventing uneven Sb metal segregation to the cap/oxide interface. For full details of this work, please see the publication based-on this work (Appendix).

We note that originally we had proposed to determine whether internal metal layers, such as the Sb layers realized in the lateral oxidation, could be used to enhance strain relaxation. Due to the limited duration of the program, we were unable to complete that aspect of the program. However, in a subsequent program this would be an area of possible study.

Personnel Supported:

Faculty:
James S. Speck – Materials Dept.

Graduate Students
Sheila Mathis – Materials Dept., Ph.D., 2000
A. Maxwell Andrews – Materials Dept., Ph.D. work still in progress.

Note: the contract with NC A&T provided partial support for both Sheila Mathis and A. Maxwell Andrews. The NC A&T funds supported the final thesis work of Sheila Mathis on lateral oxidation of the Al(As,Sb) and the initial thesis work of A. Maxwell Andrews in this area. The primary support for Sheila Mathis' dissertation work was from the AFOSR PRET Center at UCSB (Center for Non-stoichiometric Semiconductors, G. Witt, Program Manager). The funds from NC A&T were used for student stipend support and experimental costs (including MBE growth, cleanroom charges, and characterization (x-ray diffraction, AFM, TEM)

Publications (attached):

"Lateral oxidation kinetics of AlAsSb and related alloys lattice matched to InP", S.K. Mathis, K. H.A. Lau, A.M. Andrews, E.M. Hall, G. Almuneau, E.L. Hu, and J.S. Speck, *J. Appl. Phys.* **89**, 2458 (2001).

III. PUBLICATIONS & THESIS ARISING FROM AFOSR

Refereed Publications

T. A. Rawdanowicz, S. Iyer , W. C. Mitchel, A. Saxler and S. Elhamri "Electronic properties of heteroepitaxial undoped and n-InSb epilayers using SnTe source by molecular beam epitaxy" To be published in June Issue of J. Appl. Phys.

S. Iyer, S. Mulugeta, W. Collis, S. Venkatraman, K. K. Bajaj and G. Coli, "Photoreflectance Studies of Te-Doped GaSb at the $E_0+\Delta_0$ Transition", J. Appl. Phys. 87, 2336-39 (2000).

Non-refereed Publications and Presentations

S. Iyer, D. Jones and R. Dawson, " MBE Growth of GaSb on GaAs with InSb Interlayer", Amer. Phys. Soc. Spring Meeting , SanFrancisco, CA, April 16, 2001

S. Iyer, S. Mulugeta, W. Collis, K.K. Bajaj, G. Coli "Photoreflectance Studies of Te-doped GaSb", American Physical Society Spring Meeting, Minneapolis, MN, March 23, 2000

S. Iyer, S. Mulugeta, K.K. Bajaj, , J. Li, S. Venkatraman and B. Mangalam, " Characterization of Te-Doped GaSb at the Spin-Orbit Split Transition using Electromodulation Spectroscopy", American Physical Society Spring Meeting, Los Angeles, CA, March 17, 1998.

Other Presentations

S. Iyer "Compliant Substrates for MWIR" at Progress in Semiconductor Detectors Conference sponsored by AFOSR @ Williamsburg, VA 4th Jun.2001

S.Iyer, "Research at NCA&TSUon Antimonide Based Compound Semiconductors" Invited Speaker at NC Section of the MRS, MCNC Nov.10, 2000.

S. Iyer, " Growth of Sb Based Compounds and Characterization, AFOSR Program Review, Dayton, Ohio, 29th Sept. 1999.

S. Iyer, "Electrical Properties of MBE Grown Undoped and Doped InSb/GaAs using SnTe Source", - MBE User's Group Meeting, NIST, Gaithersburg, MD, 27th Oct. 1998.

Publication in Preparation

"A Comprehensive Study of GaSb Epilayer grown on InSb Compliant Layer"

Graduate Degrees Awarded

"Study of Different Interlayers in GaSb Growth on GaAs using Molecular Beam Epitaxy", Liangjin Wu, 05/02

Photoreflectance Study of Te-Doped GaSb at the E_0 Transition, Baohong Gong, 9/99

Undergraduate Projects

David Jones, (Winner of MRS -Undergraduate Materials Research Initiative)" A Novel Approach to Lattice Engineered Substrate" , 2001

Carla Ford, (Participant of NASA-Summer Undergraduate Research Experience Program),"X-ray Diffraction Measurements of Semiconductors". 2000

IV. PARTICIPATING SCIENTIFIC PERSONNEL AND REPORTS SUBMITTED (Revised)

Faculty

Dr. Shanthi Iyer, Professor

Post Doctoral Research Assistant
Dr. Jia Li

Graduate Students

Mr. Solomon Mulugeta, was a Ph.D. candidate
Mr. Yusuf Farah, was a MSEE candidate
Mr. Sreenivasan Venkatraman, was a Ph.D. candidate
Mrs. Baohong Gong, MSEE
Mr. Ilyan Sezanayev, was a MSEE candidate
Mr. Otto Burston, was a MSEE candidate
Mrs. Liangjin Wu, MSEE

* Many of the graduate students did not complete the program as they all got a well paid job due to the better national economy during this period...

Undergraduate Students
Mr. David Jones
Ms. Cynthia Knight
Mr. Khareem Almo
Mr. Kirk Heywood
Ms. Ly Tran
Mr. Nganamakabave Ella Mokena

Collaborators
Dr.Ralph Dawson and Dr. Kevin Malloy, University of New Mexico
Dr.Subash Mahajan, Dr.Kevin Malloy & Dr.Dae-Woo Kim, Arizona State University
Dr.Jim Speck & Dr.Shiela Mathis, University of California @ Santa Barbara
W.C.Mitchel, A.Saxler & S.Elhamri, Air Force Research Laboratory
Dr.K.K.Bajaj & Dr.G.Coli, Emory University

Reports Submitted
Interim Report, 8/1/99-3/29/00
Annual Report: 8/31/98 -7/31/99
Annual Report: 3/01/98 -7/31/98

IV. PARTICIPATING SCIENTIFIC PERSONNEL AND REPORTS SUBMITTED

Faculty

Dr. Shanthi Iyer, Professor

Graduate Students

Mr. Solomon Mulugeta, was a Ph.D. candidate
Mr. Yusuf Farah, was a MSEE candidate
Mr. Sreenivasan Venkatraman, was a Ph.D. candidate
Mrs. Baohong Gong, MSEE
Mr. Ilyan Sezanayev, was a MSEE candidate
Mr. Otto Burston, was a MSEE candidate
Mrs. Liangjin Wu, MSEE

* Many of the graduate students did not complete the program as they all got a well paid job due to the better national economy during this period...

Undergraduate Students
Mr. David Jones
Ms. Cynthia Knight
Mr. Khareem Almo
Mr. Kirk Heywood
Ms. Ly Tran
Mr. Nganamakabave Ella Mokena

Collaborators
Dr.Ralph Dawson and Dr. Kevin Malloy, University of New Mexico
Dr.Subash Mahajan, Dr.Kevin Malloy & Dr.Dae-Woo Kim, Arizona State University
Dr.Jim Speck & Dr.Shiela Mathis, University of California @ Santa Barbara
W.C.Mitchel, A.Saxler & S.Elhamri, Air Force Research Laboratory
Dr.K.K.Bajaj & Dr.G.Coli, Emory University

Reports Submitted
Interim Report, 8/1/99-3/29/00
Annual Report: 8/31/98 -7/31/99
Annual Report: 3/01/98 -7/31/98